University of Stavanger

Faculty of Science and Technology

MASTER'S THESIS

Study program/Specialization: Petroleum Engineering Specialization: Well Engineering	Spring semester, 2016 Open access
Writer: Tor David Østvold	…… (Writer's signature)
Faculty supervisor: Jan Aage Aasen External supervisor(s):	
Thesis title: Increasing Temperature Range of Geothermal Production Casing by Mechanical Pre-tensioning	
Credits (ECTS): 30	
Key words: Mechanical pre-tensioning, pre-tensioning, geothermal, drill string, buckling, high temperature, production casing, inner-string cementing, casing failure	Pages: 68 + enclosure: 0 Stavanger, 15-06/2016 Date/year

Master Thesis
PETMAS

Increasing temperature range of geothermal production casing by mechanical pre-tensioning

Universitetet
i Stavanger

Tor David Østvold

University of Stavanger

June 15, 2016

Acknowledgements

I would like to express my sincere gratitude to Associate Professor at UiS, Jan Aasen, for his supervision, creative ideas, helpful input, long prosperous discussions, and being available on e-Mail any day of the week. His educational approach of explaining complex problems in a simple manner made it that much easier to understand complex matters.

I would also like to express my sincere gratitude to my father Arnold Østvold for hearing out my ideas and concerns, for always coming up with helpful and eye-opening input, and for proof-reading this thesis.

I would also like to thank my family, and especially my co-habitant, Inger-Johanne Ravndal, for their continuing support during the period of writing this thesis.

Abstract

Thermally-induced forces in a fully cemented geothermal production casing can cause compressive failure during production of high temperature formation fluids. These failures lead to production downtime and costly repairs. The compressive forces can be mitigated by applying a pre-tension load on the casing during the cement curing period. The pre-tension method presented in this thesis is a new technique which consists of applying a drill string weight on the casing through mechanical slips during the cement curing period. A representative case study was constructed to test the feasibility of the method and to reveal the axial performance of both casing and drill string, and corresponding effects on well design, before and after the application of the pre-tension load. Analyses show that neither the casing nor the drill string yields during the pre-tensioning operation, and an increased temperature range of the casing during production is achieved. As pre-tension forces reduce the threshold of tensile failure in the casing, some care must be exercised when cooling down the well.

Table of Contents

List of Figures

List of Tables

Nomenclature

Below follows three lists of abbreviations, symbols, and subscripts that are frequently used in this thesis. The symbol list must be combined with the subscripts to make sense. As an example, the symbol A_o, dc refers to the outer area of the drill collars, while A_i, dp refers to the inner area of the drill pipe.

Abbreviation	Explanation
ppg	pound per gallon
sg	specific gravity
ppf	pound per foot
DF	Design factor
API	American Petroleum Institute
FEA	Finite element analysis
TWC	Thick-walled cylinder
TDS	Total dissolved solids
CaP	Calcium aluminate phosphate
SAE	Styrene acrylic emulsion
PDC	Polycrystalline-diamond-compact
RPM	Revolutions per minute
ROP	Rate of penetration
WOB	Weight on bit
BHA	Bottom-hole assembly
ECD	Equivalent circulating density

Symbol	Explanation	Value/Unit
F	Force	lbf
FR	Real force	lbf
FE	Effective force	lbf
F_f	Buckling force	lbf
Q	Pre-tension force	lbf
σ_t	Tangential stress	psi
σ_r	Radial stress	psi
σ_a	Axial stress	psi
σ_b	Bending stress	psi
σ_z	Total axial stress	psi
τ	Shear stress	psi
σ_{VME}	Von Mises stress	psi
σ_y	Yield stress/strength	psi
σ_T	Thermal stress	psi
P	Pressure	psi
E	Modulus of Elasticity	$30.45 \cdot 10^6$ psi
T	Temperature	°C
$\triangle T$	Temperature differential	°C
α	Thermal expansion coefficient	$12 \cdot 10^{-6} \frac{1}{°C}$
w	Weight per unit length	ppf
ρ	Density	ppg or sg
K	Parameter in friction analysis	$\frac{1}{lbm \cdot in}$
L	Length	ft or in
z	Well depth coordinate	ft or in
n	Neutral point	ft or in
OD	Outer diameter of tubular	in
ID	Inner diameter of tubular	in
r	Radius of tubular	in
t	Wall thickness	in
R	Tubular-to-casing radial clearance	in
A	Area of tubular	in^2
I	Moment of Inertia	in^4
f	Friction factor	Dimensionless
OD/t	Slenderness ratio	Dimensionless

Subscript	Explanation
i	Inside of tubular
o	Outside of tubular
s	Steel
dc	Drill collar
dp	Drill pipe
c	Casing
cc	Casing coupling
y	Yield
T	Thermal
pt	Pre-tension
crit	Critical
H	Heating
C	Cooling
Max	Maximum value

Chapter 1

Introduction

High temperature geothermal wells are at the risk of yielding. This is due to a rapid heat-up of production casings once hot formations fluids are produced through such casings (Southon 2005). As geothermal wells are usually cemented to all the way to surface (Nelson & Guillot 2006), any rise in well temperature from above the reference temperature when the cement sets, gives rise to compressional forces in the cemented casing (Southon 2005). Rapid heat-up therefore results in compressional failure and causes the casing body to yield, followed by thread jumps in nearby buttress threaded connections (Southon 2005). Once yielded, the cannot contain pressure and is subject to uncontrolled leakage of produced fluids. This leads to production downtime and costly repairs (Southon 2005).

These compressional forces can be mitigated by pre-tensioning the production casing (NZS 2403:2015 2015) (Li 2008) (Southon 2005). Li (2008) proposes a method which induces tension in the casing by pre-pressuring the casing during the cement solidification period. The method is developed for cyclic steam injection wells that experience the same failure mode in production casings during the hot steam injection phase of the well. For a different although similiar application, petrowiki.org (2015) suggests to apply a pick-up force when landing the casing in the surface wellhead to avoid buckling. This approach is intended for oil and gas wells which are not fully cemented to surface, but the technique can also be utilized to pre-tension the casing for thermal applications. Southon (2005) refers to the benefits of pre-tensioning a casing and the possibility of applying a pre-tension load when the casing string is stage cemented. Alongside Huenges & Ledru (2011) and NZS 2403:2015 (2015), Southon barely goes into detail on how the pre-tension load is applied. Magneschi et al. (1995) performed an analysis on imperfectly cemented portions of a casing in the presence of thermal stress and an axial load. If applying a pre-tension load to the casing, it was concluded that the casing could allow longer sections of poor cement before critical buckling loads would cause failure. However, the benefits were to difficult to achieve as the necessary preloads were too large, and because of the practical difficulty of applying them.

Based on the failure mechanism described above, the benefits of applying a pre-tension load on the casing, and the lack of well-defined mechanical pre-tension methods, the objective of this thesis is to introduce, develop, visualize, and test a novel pre-tensioning method consisting of setting down a drill string weight on slips, which are engaged into the inner wall of a geothermal production casing during the cement curing period. For the case study defined in Chapter 5, a maximum pre-tension load of 211000 lbf (95.7 metric tons) is achieveable. The pre-tension on the casing increases the temperature range within which the casing can safely operate during production without inducing compressional failure.

Chapter 2 introduces the topic of geothermal energy and explains how geothermal wells are constructed.

Chapter 3 explains pre-existing pre-tensioning methods. The newly developed pre-tensioning method, which involves use of the drill string, is also explained and shown in the figures.

The new and developed pre-tensioning method by use of drill string is also explained and visually presented by figures.

Chapter 4 includes relevant theory and equations necessary to perform drill string and casing analyses.

Chapter 5 presents the constructed case study with accompanying analyses, results and discussions.

Chapter 6 provides a conclusion on the evaluation of the drill string method, along with key findings and results.

Chapter 2

Geothermal well construction

The main goal of this chapter is to introduce the reader to the topic of geothermal energy, and geothermal well construction. As the topic is extensive, the scope has been narrowed down to include the necessary information required to create a representative geothermal case study. This case study (Chapter 5) will then be used to evaluate the feasibility of the developed pre-tensioning method (Chapter 3).

2.1 Brief introduction to geothermal energy

Geothermal energy is heat (thermal) extracted from the Earth's (geo) interior in the form of high-temperature water and/or steam. The main natural mechanisms which generate these thermal conditions can be shortly comprised to (Huenges & Ledru 2011):

1. Magma intrusion from the Earth's mantle into the crust
2. Radioactive minerals
3. Highly exothermic reactions between rock minerals, for example serpentization.

According to eia.gov (2015), there are three main types of geothermal energy systems:

1. Direct use and district heating systems use hot water from springs or reservoirs located near the surface of the earth. Direct use heating systems are utilized for bathing and cooking, while district heating systems are used for heating buildings.
2. Electricity generation power plants require water or steam at high temperatures (approximately 150°C to 370 °C). Geothermal power plants are generally buit where geothermal reservoirs are located within a mile or two of the surface of the Earth (1.6 - 3.2 km).
3. Geothermal heat pumps use stable ground or water temperatures near the Earth's surface to control building temperature above ground.

With the above points in mind, it is clear that geothermal energy is normally exploited within the range of a few meters to several kilometers into the subsurface of the Earth, and the temperature span encountered usually lies between 30 to 370 °C. Interestingly, the world's hottest well to date was reported to hold a temperature of 450°C (Friðleifsson et al. 2015).

Geothermal energy is a natural step forward for the oil and gas industry due to many similarities between the geothermal industry and the oil and gas industry. Both energy

systems are built up by subsurface reservoirs that are generated by natural geological processes and may contain fluids that are energydense due to high-temperature or chemical composition, and are mainly accessed through drilling wells made up of steel tubulars. The expertise and knowledge from the petroleum industry is invalueable to the extraction of high-temperature geothermal resources. Similarly, the expertise and knowledge from the geothermal industry is also invalueable to the extraction of petroleum reseources due to increasingly harsher well conditions as conventional hydrocarbon resources are depleted.

Geothermal energy is an attractive energy resource due to its renewable nature, cheap utilization, little pollution, and is an "extremely reliable source of power" (Thorhallsson 2003). If geothermal wells are allowed to produce continuously, geothermal energy is considered to be more reliable than other renewable energy sources, including solar sources, wind sources and hydroelectric power. These other energy sources are dependent on the weather and seasonal variation and they are therefore less reliable.

Generally speaking, the temperature through the Earth's crust increases with depth, regardless of location. This is referred to as the geothermal gradient. The value of the geothermal gradient, however, is highly dependent on the specific location. In theory this means that geothermal energy can be extracted almost anywhere in the world, as long as the well is deep enough. Please observe, however, that there must be a geothermal reservoir present to exploit, and specific criteria must therefore be met. These criteria are(H. Dickson & Fanelli 2004):

1. Presence of a heat source
2. Presence of a subsurface water reservoir
3. Presence of a permeable reservoir rock

The presence of a heat source is usually fullfilled as the Earth itself is a heat source. Utilizing high-temperature reservoirs by drilling deep in average geothermal conditions (2.5-3°C/100m) with current technology would, however, be devastatingly expensive and would therefore not be economically feasible (H. Dickson & Fanelli 2004). For this particular reason, high-temperature geothermal energy is usually extracted in areas with higher-than-average geothermal gradients (H. Dickson & Fanelli 2004). These areas are located near tectonic plate boundaries, which are shown in the following figure. Italy, Iceland, USA, Hawaii, New Zealand, and The Phillipines represent some of the areas with above-average geothermal gradients.

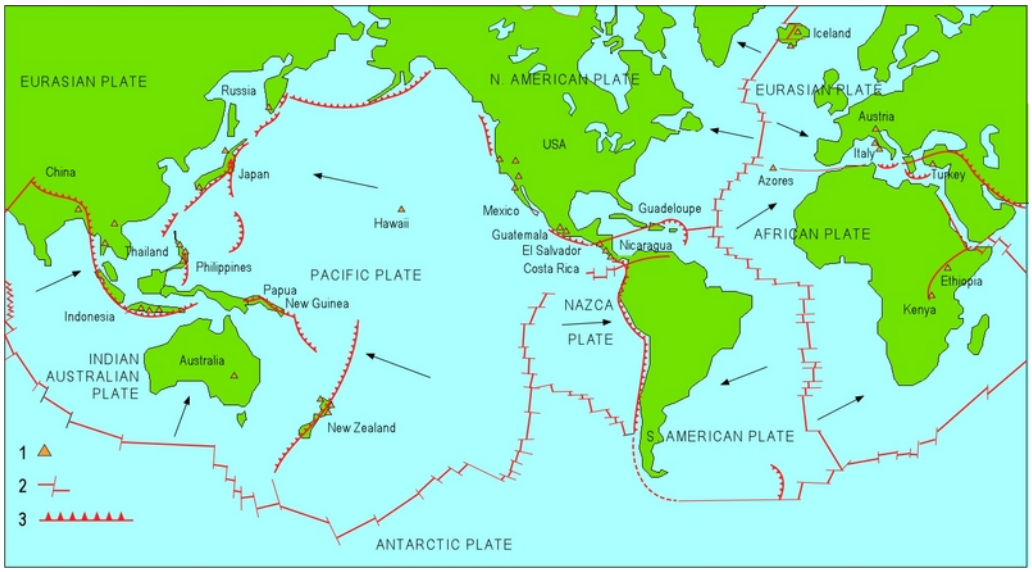

Figure 2.1: Map showing the tectonic plate boundaries of the world. Yellow triangles represent geothermal fields producing electricity (H. Dickson & Fanelli 2004).

2.2 Nature of geothermal formations

Geothermal formations are, by definition, hot, often hard, abrasive, highly fractured, and under-pressured (below the water gradient). They often contain corrosive formations fluids, such as brines with high TDS (total dissolved solids) content, and dissolved or free CO2 (carbon dioxide) and H2S (hydrogen sulphide) gases. These conditions mean that drilling geothermal wells is time-consuming due to rapid bit wear and low rate of penetration (ROP); corrosion of casings and surface production equipment lead to costly repairs and/or failures; lost circulation is frequent and severe; and most of these problems are further amplified by high temperature (Finger & Blankenship 2010).

2.3 Rotary drilling

Drilling geothermal wells is nearly identical to the approach used in the petroleum industry. Geothermal reservoirs are reached by rotating a drill string in a downward motion through various formations. Other methods exist, but will not be pursued here. The drill string consists of suitable drill pipe, thick-walled drill collars, jars, and other necessary downhole tools. And, of course, the drill bit. Roller-cone and polycrystalline-diamond-compact (PDC) bits are normally used. Roller-cone bits are the preferred choice due to their durability in hard and fractured rocks that are characteristic for geothermal reservoirs (Finger & Blankenship 2010). In recent years, however, significant progress has been made for PDC bits, and they are slowly becoming accepted by the geothermal industry.

The shearing action of PDC bits is inherently more efficient to progress through formations than the crushing action of roller-cone bits (Finger & Blankenship 2010). However, this is not

the main reason for the increasing interest of PDC bits in geothermal applications. It is the bit wear performance under high temperatures. The PDC bits do not have any moving parts, therefore temperature limitations on bearing, seals, and lubricant are not a factor (Finger & Blankenship 2010).

As geothermal formations tend to be under-pressured, reducing drilling mud density by injecting compressed air or nitrogen into the circulation system is utilized. This reduces lost circulation during drilling, and reduces wellbore skin damage (Birkisson & Hole 2006). The prevention of lost circulation is also the greatest disadvantage as "aerated drilling prevents the loss of drilling fluid to the formation and thus reduces the cooling of the formation and near well bore formation fluids" Birkisson & Hole (2006). This leads to higher circulating temperatures. Therefore, in high temperature aerated drilling of medium formations (medium relates to the compressive strength of formation), PDC bits have been rerun up to 4 times the drilled length than that of roller-cone bits (Finger & Blankenship 2010).

2.3.1 Drilling fluid density

A wide range of drilling fluid densities are used depending on field-specific details and applications. According to Finger & Blankenship (2010), typical densities are between 1.03 and 1.15 sg (specific gravity). Lower densities are obtained by injecting air or nitrogen into the fluid. The lower limit of aerated water and bentonite mud is 0.3 and 0.4 sg, respectively (Birkisson & Hole 2006). Drilling with air (0.03-0.05 sg Birkisson & Hole (2006)) is also relatively common, but is mainly used in dry hard rock where borehole stability is not a problem (Huenges & Ledru 2011). Borehole stability covers a wide range of problems, but can be comprised to mechanical and chemical changes in the drilled formations that affect the size of the wellbore during and after drilling. Based on the above information, it can be concluded that common drilling fluid densities used for geothermal wells range from 0.03 to 1.15 sg.

2.4 Casing design

From an overall perspective, two types of casing designs are utilized in geothermal wells. These designs consists of the stress-base design and the strain-based design (NZS 2403:2015 2015). The maximum limit for a stress-based design is the casing material yield strength. This type of design is widely used in the petroleum industry. The maximum limit for a strain-based design is governed by the ductility of the material, and is usually set as a maximum allowable strain limit. As temperature is the parameter that governs failure in geothermal wells the most, and pressures are usually low, the casing may exceed its yield strength without compromising the integrity of the well. Strain-based designs are more complex as the material behaves non-linearly once yielded. FEA (Finite Element Analysis) is usually required to design a well by strain.

2.4.1 Casing grades, size, and connections

In general, steel casings used for geothermal application are "standardized". The most common standard is the "API Specification 5CT" from the American Petroleum Institute (Huenges & Ledru 2011). In situations where gas may be present (which is usually the case for geothermal wells), casing materials should be selected to minimize the possibilities of failure by hydrogen embrittlement or by sulphide stress corrosion (NZS 2403:2015 2015). API grade steels which provide resistance to H2S attack are (NZS 2403:2015 2015): H40, J55, K55, M65, L80 type 1, C90 type 1, and T95 type 1. According to Hole (2008), casing grades K55 and L80 are typically utilized, and API buttress threads have been found to be suitable. Typical outer diameters of geothermal production casings are: 13⅜", 10¾", and 9⅝" (Southon 2005).

2.4.2 Casing cementing

Many methods are used to cement a casing, but only one method is of interest for this study. The inner-string cementing technique is explained and visualized in Chapter 3.

Geothermal casings are almost always cemented to surface. If the cement job leaves a tightly gripping cement sheath (with low permeability) along the full length and circumference of a casing, the cement sheath should (Holligan et al. 1989) (Thorhallsson 2003):

- prevent buckling of casing due to thermal expansion during production:
- prevent annular corrosion of casing by minimizing channeling in the cement:
- prevent annular fluid expansion during production as all liquids present in the annulus prior to the cementing operation have been displaced.

It is critical that the casing is supported by good cement as most casing failures are directly, or indirectly, related to the cement job. This is made clear in the following section.

As most casing failures are directly or indirectly related to the cement job, it is critcal that the casing is supported by good cement (Nelson & Guillot 2006) (Thorhallsson 2003).

2.4.3 Casing failures

The most common failure mechanisms in geothermal wells are, generally, attributed to corrosion and high-temperature (Southon 2005). Trapped annular fluid expansion is the main cause of casing collapse, and may be a result of poorly displaced annular contents during the cement job, or poor cement quality (Thorhallsson 2003). When the well is heated up during production, this heat causes the trapped annular fluid to expand within a confined space. This results in high pressure, usually leaving the innermost casing in collapse mode.

The casing failure which is of most focus in this thesis is related to the rapid heat-up of geothermal production casings once hot formation fluids are brought into production. This failure mechanism has been adequately described in the Introduction.

Other casing failures are beyond the scope of this thesis, and will therefore not be mentioned here. Interested readers are referred to Southon (2005).

2.4.4 Starting wells

As geothermal formations tend to be under-pressured, the wells need to be "kickstarted" artifically . In Iceland, this can be accomplished by introducing compressed air into a closed well. The compressed air pushes the water content down in the well, causing it to enter the formation where it is heated to in-situ temperatures. The well is rapidly opened once the temperature of the water reaches a critical level. The water will spontaneously boil and cause enough steam "air lift" for the well to flow (Thorhallsson 2003). Many other methods exist, but they will not be mentioned here.

Well killing is covered in sub-section 4.3.2.

2.4.5 Measures to extend well life

According to Thorhallsson (2003), the following simple steps can assure the longevity of producing geothermal wells:

1. Keep well killing to a minimum, and keep the well hot and in production. This reduces the thermal cycling load on the well, which is the main contributor to failure in geothermal wells (Hole 2008).
2. Seal any leaks as soon as they appear. Leaks are worsened with time, dealing with them early is good practice.
3. Corrosion in the topmost part of the well is usually the most severe failure (Thorhallsson 2003). Corrosion can be prevented by keeping the area (cellar) around the wellhead dry. In this context, a cellar is basically a cube-shaped excavated hole within the first few meters of the ground with lined walls of cement. The cellar "accomodates part of the wellhead and assist in managing drilling mud or water around the wellhead during drilling and throughout the life of the well" NZS 2403:2015 (2015).

Chapter 3

Methodology

3.1 Existing pre-tensioning methods

The concept of pre-tensioning casings in thermal applications is known in the industry. Oftentimes pre-tensioning is performed to avoid thermally induced buckling in uncemented casing lengths (Huenges & Ledru 2011). For casing strings that are fully cemented to surface, and for which buckling is no longer a concern, pre-tensioning is performed to reduce compressive stresses due to heating from produced hot fluids (NZS 2403:2015 2015). Pre-tensioning can be achieved by applying a pick-up force on the casing after casing is cemented and anchored in place (petrowiki.org 2015). Before pre-tensioning the casing, however, one must ensure that the additional tensile force does not exceed the tensile strength of the casing or cement, as this can cause serious well failure.

As opposed to achieve pre-tension by mechanical means, Li (2008) proposes to exert an internal pressure on the casing during the period of solidifying the cement. As the casing is free to move, the applied pressure expands the casing radially and axially so as to induce tension hydraulically. This effect is known as ballooning (Bellarby 2009). The method is as follows: Cement is pumped into the casing annulus by conventional means. Shortly after, drill pipe is run down to the casing section adjacent to a pay-zone, where a packer is activated to isolate the volume between the packer and the bottom of casing. A highly pressurized fluid is circulated down to the isolated volume between the packer and the bottom of casing, and high pressure is maintained throughout the solidfication period.

Li's calculations show that, when using this method, higher safety factors are obtained throughout the production life cycle and no plastic deformation occurs. Although the theoretical results are good, there are some practical disadvantages to this method. Once the pre-pressurization is complete and the internal pressure is removed, the casing will contract (reverse balloon). This contraction of the casing generates microannulus between the casing and the cement sheath. This may produce potential leakage paths for fluids during the production phase, but the microannulus could also disappear once pressure is applied again. This method is intended for cyclic steam stimulation wells (in Li's words: thermal recovery wells), where the well is used periodically as a conduit for injection of steam, and is also used periodically as a conduit for production of heavy crude oil.

For the case defined in Li (2008), calculations were based on application of internal pressures ranging from 0 - 50 MPa (0 - 500 bar). Even for pre-pressures below 30 MPa, the 7 inch N-80 casing exceeded the yield limit due to thermal stress. Pressures seldomly exceed the water

gradient in most geothermal applications (Nelson & Guillot 2006). For this reason (among others) it is common and sufficient to use K-55 casing for production purposes (Finger & Blankenship 2010). Inducing pre-pressures above 30 MPa could be detrimental for lower grade production casings, such as K-55 casings. It can also prove difficult to maintain high pressure over a longer period of time without inducing leakage paths, or any pressure inconsistencies.

3.2 Mechanical pre-tensioning of casing using the drill string

Considering the use of lower grade casings in geothermal wells and the practical disadvantages of hydraulic pre-tensioning, a mechanical pre-tensioning method is more likely to prove sucessfull. As mechanical methods usually involve few components that can fail and therefore are naturally primitive, mechanical methods are generally considered to be reliable. The novel method of this thesis proposes to subject the casing to weight-induced tension at a point above the casing shoe during the cement-soldifying period.

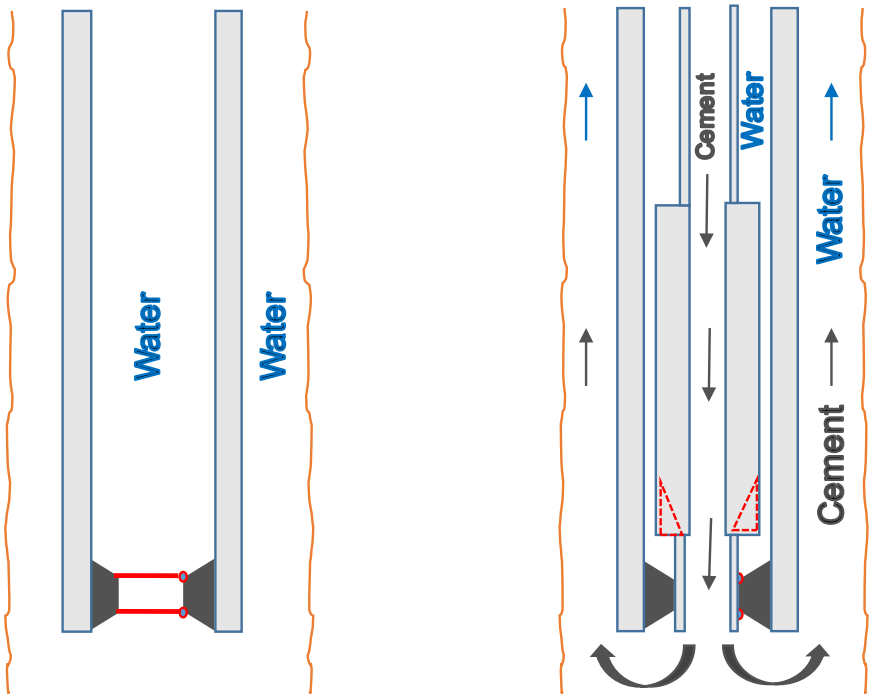

(a) Running the casing to target depth **(b)** Cementing through the drill string

Figure 3.1: Steps 1 through 4 of the pre-tensioning operation

Figures 3.1a and 3.1b show simplified cross-sections of the bottom of the well during the running and cementing of the casing, respectively. Note that the figures are not to scale. Figure 3.1a shows a casing placed in the wellbore. The white space between the casing and the wellbore is the casing-to-wellbore annulus. This annulus is initially filled with a drilling fluid, in this case water. The casing is also filled with water. A simplified float collar valve is also shown at the bottom of the casing. The float collar valve has two check-valves, represented by red lines and accompanying hinges (red/blue dots). These valves only allow fluid flow

from the inside to the outside of the casing. Heavier density cement can therefore not flow back inside the casing once placed in the casing annulus.

Figure 3.1b shows a drill string assembly which has been run back to the bottom of the well once the casing has been hung off in the wellhead. From top to bottom, the drill string is built up by drill pipe, thick-walled drill collars, and a stab-in sub at the bottom. The stab-in sub enters the float collar valve and allows fluid communication between the casing annulus and an inner drill string. Dotted triangles represent retracted and inactive mechanical slips. These are located at the bottom of the drill collar section. Cement is pumped through the drill string and then up the casing annulus. The cement gradually displaces the water. The inside of casing is filled with water throughout the operation. This part of the method is known as the inner-string cementing technique. The details are based on figures and information provided by Nelson & Guillot (2006).

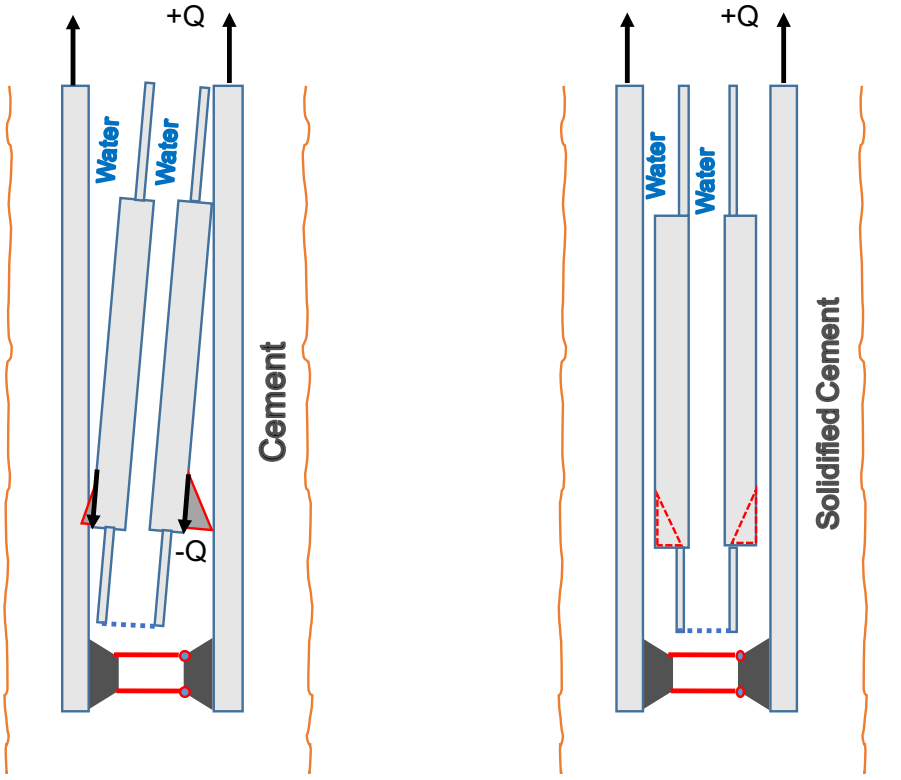

(a) Pre-tensioning of the casing **(b)** Pulling back the drill string

Figure 3.2: Steps 5 through 8 of the pre-tensioning operation

Figure 3.2a shows the cement once properly placed in the casing annulus, and after the drill string has been disconnected and pulled back a few feet from the float collar valve. Here, mechanical slips are shown activated and engaged into the inner casing wall. Once fixed to the inner casing wall, the whole weight of the drill string is reduced by slacking off weight at the surface. Pre-tensioning load +Q is therefore transferred to the casing through the mechanical slips engaged to the inner casing wall, thereby subjecting the drill string to a slack-off load -Q. This will initiate buckling of the drill string. The weight of the drill string

is kept on the slips through the entirety of the cement curing period.

Figure 3.2b shows the cement once solidfied, and after the drill string has been brought back into tension, slips have been deactivated, and the drill string is being pulled back to surface. The casing is now subjected to a pre-tensioning load +Q. The procedure of the method is concisely summarized in the following eight steps:

1. After drilling the $12^1/_4$" hole section, run the $9^5/_8$" casing to target depth, and hang off in the wellhead.
2. Run the $5^1/_2$" drill string to the bottom of the casing.
3. Stab the drill string into the float collar valve inside the casing.
4. Pump cement through the drill string, and up the casing annulus. Continue pumping until cement returns are observed at surface.
5. Unlatch the drill string and pull back a couple of feet, then activate the mechanical slips.
6. Slack-off the drill string to transfer weight-induced tension to casing through the slips.
7. Keep the weight on slips through the cement curing period.
8. Once the cement has set, pull the drill string back into tension, deactivate the slips, and pull back the drill string.

A series of assumptions and requirements are necessary to exemplify the use of this method. As the method requires application of a pre-tension load during the cement curing period, the cement job most likely has to be performed in one stage due to time constraints. In practical terms this means that the cement must be pumped through the drill string, and major cement losses must be avoided to allow the whole casing annulus to be filled with cement at once. The latter requirement is perhaps the greatest challenge to overcome, as geothermal formations tend to have low fracture gradients (Nelson & Guillot 2006). This necessitates the use of low-density cement systems. Great care must be exercised in preventing the effective circulating pressure from exceeding the fracture strength of the formation in question. In other words, drill string back-pressure and cementing flow rates must be kept below critical levels.

Once the cement job is complete and the drill string is positioned correctly, the mechanical slips will engage and connect the drill string to the casing. The weight of the drill string is slacked off at surface, whereby the drill string goes form tension to compression. The compressive force induces spiralling into the drill string, also known as helical buckling (Bellarby 2009). It is assumed that the measured slack-off force at rig level equals the pre-tensioning load on the casing. This means that any friction generated from contact forces between the buckled drillstring and the hanging casing only serves to distribute pre-tensioning load along the casing wall. In mathmatical terms, the sum of friction forces plus the weight on the slips equals the casing pre-tensioning load.

It is assumed that the cement, once set, is sufficiently strong to tolerate the additional tension without failing. Under this assumption, the further analysis focus on establishing the limits of

the drill string under the buckling load, and the limits of the casing under the pre-tensioning load. Further evaluation and discussion will reveal the feasibility of this method and the corresponding effects on well design. This will be covered in Chapter 5.

Chapter 4

Theory

All symbols and parameters used in this chapter are defined in the initial nomenclature section. Some symbols and definitions, however, are explained in this chapter.

4.1 Effective and real force

Stress calculations are based on force as an input parameter. In relevant stress calculations, the *effective force (FE)* and *real force (FR)* are of particular interest. Q represents the pre-tensioning load for casing calculations, and slack-off load for drill string calculations. Q is defined as positive when any tubular under consideration is in tension, and negative when in compression. Therefore tension and compression are assigned positive and negative values, respectively. As functions of wellbore vertical depth, z, effective force (equal to the negative of the Lubinski et al. (1962) fictitious force) and real force are defined as follows:

$$FR(z) = Q + w_s(L - z) + A_i P_i(L) - A_o P_o(L) \tag{4.1}$$

$$FE(z) = FR(z) - A_i P_i(z) + A_o P_o(z) \tag{4.2}$$

For any well represented by the depth-coordinate (z), z = 0 represent the top of the wellbore, and z = L represents the base of the wellbore.

4.2 Stresses

All stress formulae are intended for thick-walled cylinders (TWC). Several definitions of thin-walled cylinders exist. According to Shigley (2011): "When the wall thickness of a cylindrical pressure vessel is about one-tenth, or less, of its radius, the radial stress that results from pressurizing the vessel is quite small compared with the tangential stress". This is often the assumption for calculations based on thin-walled cylinders, that the radial stress ≈ 0. In mathematical terms, thin-walled cylinders are defined by: $t < 0.1r_i$, where t = wall thickness, and r_i = inner radius. TWC must then be defined by $t > 0.1r_i$. The slenderness ratio, also known as OD/t-ratio, is used to evaluate the collapse performance of tubulars. As such, a more useful definition of TWC follows: $\frac{OD}{t} \leq 22$.

4.2.1 Hoop and radial stress

Hoop stress, also known as the tangential or circumferential stress, is the stress which acts along the wall circumference of a cylinder. Radial stress is the stress which acts in the radial direction across the wall of the cylinder. Timoshenko & Goodier (1970) derived the tangential and radial stress from Lames solution, and are defined as the following, respectively:

$$\sigma_t = -\frac{A_i A_o (P_o - P_i)}{A_s} \cdot \frac{1}{r^2} + \frac{P_i A_i - P_o A_o}{A_s} \tag{4.3}$$

$$\sigma_r = \frac{A_i A_o (P_o - P_i)}{A_s} \cdot \frac{1}{r^2} + \frac{P_i A_i - P_o A_o}{A_s} \tag{4.4}$$

where r represents the radius through the cylinder wall: from inner to outer radius. For cases without bending, the greatest stress state will occur at the inside wall as shown by Lubinski et al. (1962).

4.2.2 Axial stress

Axial stress is the stress which acts in the axial direction through the wall thickness of a cylinder. Axial loads can be induced by pressures, temperature, and weight of tubulars. The axial stress is calculated with real force as input (see equation 4.1):

$$\sigma_a = \frac{FR(z)}{A_s} \tag{4.5}$$

4.2.3 Bending stress

Bending can be caused by wellbore curvature (drilling doglegs) and by buckling (Bellarby 2009). Bending stresses arise once tubulars make mechanical contact with another solid interface, for example: contact between wellbore and drill string during drilling, or contact between casing and wellbore during running of casing. As the casing is free to move at the shoe during the cementing operation, and the case herein is for a vertical well, neither wellbore curvature nor buckling of casing will occur. Bending stresses can therefore be neglected for the casing calculations. For the drill string calculations, however, the buckled drill tring induces bending stresses. According to Lubinski et al. (1962), the bending stress due to helical buckling is calculated with effective force as an input parameter (see equation 4.2):

$$\sigma_b = \pm \frac{OD \cdot R}{4I} \cdot FE(z) \tag{4.6}$$

Note that R represents the tubular-to-casing radial clearance.

4.2.4 Total axial stress

The total axial stress is calculated as a combination of axial stress and bending stress:

$$\sigma_z = \sigma_a \pm \sigma_b \tag{4.7}$$

The '±' sign is because bending stresses are tensile (positive) on the outside of the bend, whilst being compressive (negative) on the inside of the bend (Bellarby 2009). Under combined loading of pressures and buckling, yielding may start at either side of the bend (Lubinski et al. 1962). It must therefore be established which combination creates the worst-case loading scenario, and then use this as an input parameter in the calculation of the triaxial stress state.

4.2.5 Von-Mises triaxial stress

The most widely used yielding criterion is the Huber-Henky-Mises, commonly abbreviated as Von Mises equivalent or VME (Bellarby 2009). A material will yield if the VME stress exceeds the yield strength of the material. VME stress is calculated with radial, hoop, total axial, and shear stress as input parameters:

$$\sigma_{VME} = \frac{1}{\sqrt{2}} \cdot \sqrt{[(\sigma_z - \sigma_r)^2 + (\sigma_z - \sigma_t)^2 + (\sigma_r - \sigma_t)^2] + 3\tau^2} \tag{4.8}$$

where τ is the shear stress induced by torque. This parameter can safely be neglected for the casing calculations as there is little to no rotation. Some attention should be devoted to the drill string calculations, however, as it is known that helical buckling induces torque (Mitchell et al. 2003). In some cases the buckling-induced torque can exceed the make-up torque of the tubular connections, leading them to unscrew or over-torque. This is not the case for large tubulars with relatively small radial clearances, and can for this study be ignored. Equation 4.8 therefore simplifies to (Holmquist et al. 1939):

$$\sigma_{VME} = \frac{1}{\sqrt{2}} \cdot \sqrt{[(\sigma_z - \sigma_r)^2 + (\sigma_z - \sigma_t)^2 + (\sigma_r - \sigma_t)^2]} \tag{4.9}$$

4.3 Temperature-induced forces

Once the casing is mechanically fixed to the wellbore by set cement, any temperature changes from the initial condition will give rise to additional forces. For geothermal wells these temperature differentials are of significant importance. The following subsections shed light on this matter. Do note that the Modulus of Elasticity, and yield strength of material (E and σ_y, respectively) are functions of temperature. In some cases so is the coefficient of thermal expansion (α) (Bellarby 2009), but it will be assumed to be constant for this study. The temperature effect on material properties will be covered in Section 4.4.

4.3.1 Production scenario

For geothermal wells to be economic, large diameter casings and corresponding boreholes are deployed to ensure large flowrates of the intrinsically low value produced fluid (Huenges & Ledru 2011). Discharge tests of the world's hottest well to date, IDDP-1 on Iceland, showed a maximum mass flowrate in excess of 50 $\frac{kg}{s}$ of superheated steam at 450°C and 40 bar (Friðleifsson et al. 2015). At these conditions, this corresponds to an astonishing fluid flowrate of 37500 $\frac{l}{min}$ (assuming a steam density of 12.5 $\frac{kg}{m^3}$). Although most geothermal wells do not exhibit such extreme production rates, it is not uncommon to have well-flowing temperatures close to the reservoir temperature (Finger & Blankenship 2010). This is the worst case temperature differential at the wellhead, where inside temperature $\approx$ reservoir temperature, and outside temperature = average temperature in well region. Since the casing is fixed in both ends, a temperature rise ($+ \triangle T$) causes a compressive force of (Bellarby 2009):

$$F_T = -\alpha E \triangle T A_s \ ; \tag{4.10}$$

or a corresponding compressive stress (divide equation4.10 by A_s):

$$\sigma_T = -\alpha E \triangle T \ . \tag{4.11}$$

Consider now a K-55, 53.5 ppf (pound per foot) casing with yield strength $\sigma_y = 55000$ psi, and area of steel $A_s = 15.55\ in^2$. The force at which this casing yields axially can be calculated as (Bellarby 2009):

$$F_y = \sigma_y A_s \tag{4.12}$$

which, for this case, corresponds to $F_y = 855000$ lbf. Substituting F_y for F_T in equation 4.10, and solving for $\triangle T$ (neglecting the - sign), gives us the differential temperature at which the casing yields axially:

$$\triangle T_y = \frac{F_y}{\alpha A_s E} \ . \tag{4.13}$$

Assuming a thermal expansion coefficient $\alpha = 12 \cdot 10^{-6}\ \frac{1}{°C}$, and a Modulus of Elasticity $E = 30.45 \cdot 10^6$ psi, gives a $\triangle T_y$ **= 150°C**.

Note that equation 4.13 can be rewritten as following by combining equations 4.12 and 4.13, or solving for $\triangle T$ in equation 4.11:

$$\triangle T_y = \frac{\sigma_y}{\alpha E} \tag{4.14}$$

Although this equation is simpler, it will be shown in the following section why the formulation of equation 4.13 is pursued. Upon studying equation 4.14, and assuming constant α and E, it is evident that the differential temperature range a casing can be subjected to before yielding is proportional to its yield strength. Be aware, however, this is only applicable for the linear-elastic region of the material.

4.3.1.1 Pre-tensioning effect on temperature range during production

Initializing a pre-tension of casing counteracts the compressive forces that arise when the casing is heated during production. The effect of this pre-tensioning can be calculated by substituting F_y with pre-tensioning load Q in equation 4.13, resulting in the following:

$$\triangle T_{pt} = \frac{Q}{\alpha A_s E} \tag{4.15}$$

Assume a pre-tension load of 100000 lbf is applied to the casing defined in the above section. Using equation 4.15, this corresponds to a pre-tension-induced temperature increase of 17°C. This means that after the pre-tension has been applied, the casing yields at a higher temperature differential of **167°C**. The temperature differential at which the casing yields under the pre-tension load Q can be directly calculated as:

$$\triangle T_y = \frac{F_y + Q}{\alpha A_s E} \tag{4.16}$$

4.3.2 Well quenching

Well quenching, also known as well killing or cooling, is utilized to stop the production of fluids and reduce the wellhead pressure to zero. The most common method to achieve this is by closing down the well and pumping down cold freshwater (Thorhallsson 2003). Higher density fluid might be necessary if the reservoir pressure is above the water gradient. Maintenance work on the well can then be safely conducted knowing the reservoir pressure is counteracted by the hydrostatic column of cool liquid in the well. Well quenching is also a contingency plan if serious well control issues arise during the lifetime of the well.

For a casing fixed in both ends, a temperature drop ($-\triangle T$) causes a tensile force to arise, opposite of what equation 4.10 presents. A pre-tensioned casing will therefore be more sensitive when subject to cooling, as the following equation presents:

$$\triangle T_{pt} = -\frac{Q}{\alpha A_s E} \tag{4.17}$$

Again, assume that a pre-tension load of 100000 lbf is applied to the casing defined previously. Using equation 4.17, this corresponds to a pre-tension induced temperature drop of 17°C. This means that after the pre-tension has been applied, the casing yields in tension at a lower temperature drop of **-133°C**. The temperature drop at which the casing yields under pre-tension load Q can be directly calculated as:

$$\triangle T_y = \frac{F_y - Q}{\alpha A_s E} \tag{4.18}$$

4.4 Temperature effect on material properties

Materials exposed to elevated temperatures experience loss of strength (Bellarby 2009). The following table is based on NZS 2403:2015 (2015) "Table 4 - Effect of temperature on casing properties", and presents the effect of temperature on yield strength (σ_y) and Young's modulus (E) for K55/J55/L80/C90/T95 casing grades. The yield strength of materials is usually measured at $20°C/68°F$, and serving as a reference point, it is implied that $\sigma_y = \sigma_y(T = 20°C)$.

Table 4.1: Temperature effect on material properties

	K55/J55	L80/C90/T95	All grades
Temperature [°C]	Yield strength [deration factor]	Yield strength [deration factor]	E [10^6 psi]
20	1.00	1.00	30.45
100	0.94	0.96	29.73
150	0.90	0.92	29.15
200	0.90	0.90	28.57
250	0.85	0.88	28.13
300	0.80	0.85	27.55
350	0.70	0.81	26.83

Below are graphical representations of the data presented in Table 4.1. Regression lines have been added to extrapolate formulations that can be useful for further analysis.

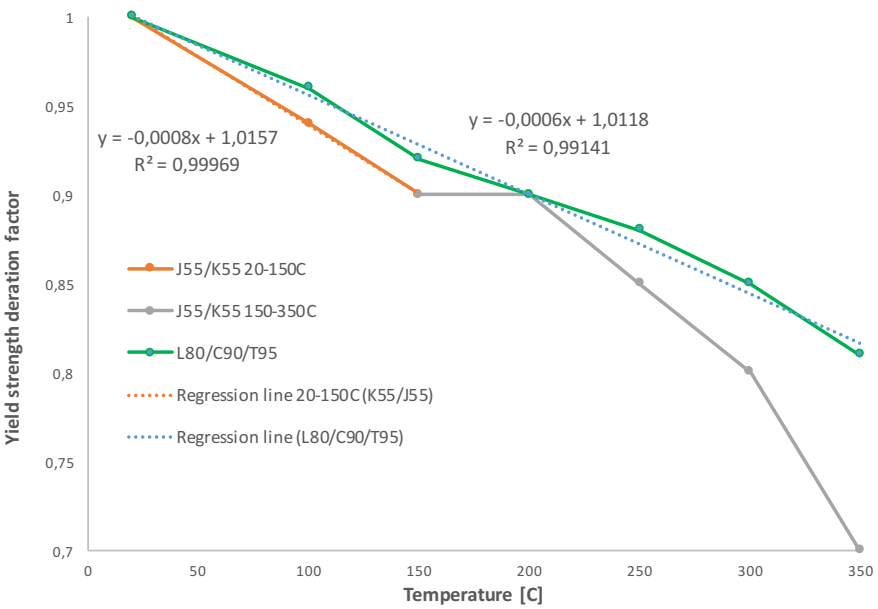

Figure 4.1: Yield strength deration versus temperature

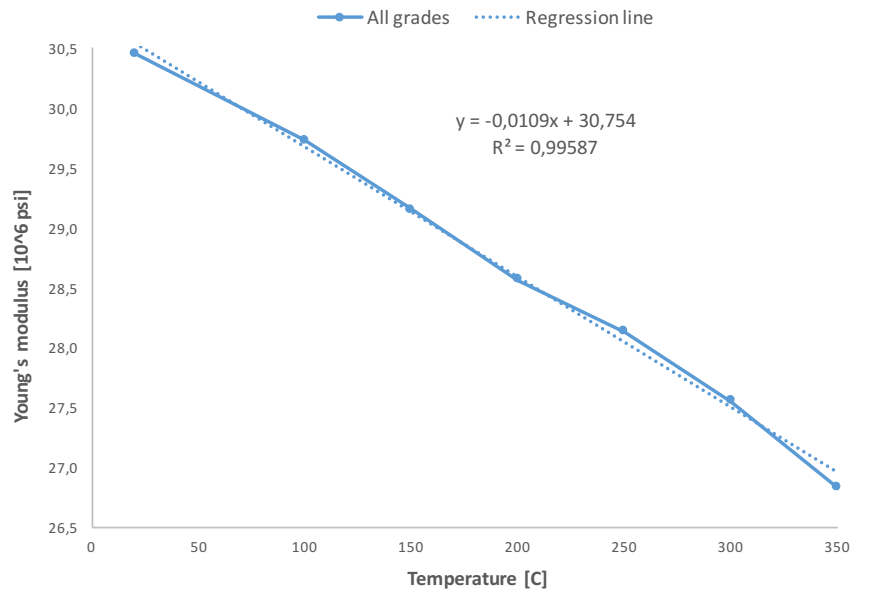

Figure 4.2: Young's modulus versus temperature

Consider Figure 4.1. A regression line for casing grades K55/J55 has only been drawn in the temperature interval of 20-150°C as there is no good linear correlation above 150°C. For casing grades L80/C90/T95, however, the regression line is nearly perfectly linear for 20-350°C. The temperature dependent yield strength for the grades in question are formulated below.

K55/J55 within temperature interval of 20-150°C:

$$\sigma_y(T) = (1.0157 - 0.0008T) \cdot \sigma_y \tag{4.19}$$

L80/C90/T95 within temperature interval of 20-350°C:

$$\sigma_y(T) = (1.0118 - 0.0006T) \cdot \sigma_y \tag{4.20}$$

Consider Figure 4.2. In this context, Young's modulus relationship to temperature can be considered linear. The following formulation can be deduced.

All casing grades within temperature interval of 20-350°C (Unit: 10^6 psi):

$$E(T) = 30.754 - 0.0109T \tag{4.21}$$

4.5 Buckling of drillstring

4.5.1 Short introduction to buckling

Once the drill string has been attached to the inside of the casing wall by mechanical slips, and followed by slacking off its weight, the drill string will start to buckle almost immediately. This is especially true for vertical wells where the drill string-to-casing drag is minimal (Bellarby 2009). Two modes of buckling are possible: sinusoidal and helical. The critical compressive force (denoted F_{crit}) required to initiate buckling in a vertical well can be calculated as the negative of what is defined in Lubinski et al. (1950).

Sinusoidal buckling:

$$F_{crit} = -1.94 \cdot (EIw^2)^{\frac{1}{3}} \tag{4.22}$$

Helical buckling:

$$F_{crit} = -4.05 \cdot (EIw^2)^{\frac{1}{3}} \tag{4.23}$$

The total buoyed weight per unit length, w, is defined as follows:

$$w = w_s + w_i - w_o \tag{4.24}$$

Consider a 8x3" drill collar with an effective (buoyed) equivalent weight , w = 10.6 $\frac{lb}{in}$ (note unit), moment of inertia, I = 197.1 in^4, and Young's modulus, E = $30.45 \cdot 10^6$ psi. The required compressive force to initiate sinusoidal and helical buckling for this case is -17000 and -35600 lbf, respectively. For the slack-off load defined in sub-section 4.3.1.1, Q = - 100000 lbf, it is evident that the drill collar is well within the helically buckled region. The next sub-section takes into account the friction which arises once helically buckled drill string comes in contact with the casing.

4.5.2 Frictional analysis of the helically buckled drill string

Prior to Mitchell (1986), helical buckle-induced friction forces in a tubing had not been considered. Mitchell defined two simplified cases in which friction was taken into account: 1) landing tubing (downward motion), and 2) tubing loaded by thermal and pressure loads (upward motion). The first-mentioned case is of particular interest for this study. Imagine the drill string being connected to the inside of the casing by mechanical slips, and is slacked-off by the force Q. The buckling force (same as the effective force), F_f, is defined by Mitchell (1986) as:

$$F_f(z) = \sqrt{\frac{w}{K}} \cdot tanh[\sqrt{wK}(z-n)] \tag{4.25}$$

where the neutral point of stability, n, is defined by:

$$n = L - \frac{Q}{w} \tag{4.26}$$

and the parameter K is defined as:

$$K = \frac{Rf}{4EI} \quad . \tag{4.27}$$

To produce F_f in pound-force, the following units must be used:

- w in lbm/inch
- n, L, z, and R in inches
- E in psi
- I in in^4

K should then be in the unit of $\frac{1}{lbm \cdot in}$.

First, consider equation 4.26. The neutral point of stability represents a depth at which the tubular is neither straight nor buckled (Lubinski et al. 1962). The tubular is straight above, and buckled below, the neutral point. Therefore, equation 4.25 is only valid from the neutral point and below this point. As there are no contact forces between the drill string and the casing above the neutral point, the buckling forces are calculated from equation 4.2. This also holds true when the friction is neglected (f = 0).

Consider equation 4.27. The K parameter introduces the coefficient of friction, f. Based on "Table 1 - Coefficients Of Friction" Mitchell (1986), Mitchell suggests a plausible range of f between 0.1 and 0.4. This range will be considered for further analysis.

A graphical visualization of the aforementioned model follows. The visualization is based on input data from Mitchell (1986) "Table 2 - Sample problem data", with a few modifications. The data is reproduced in the following table:

Table 4.2: Input data for the buckling force example

	Tubing	**Casing**
OD/ID, in	2.875/2.441	7.0/6.094
w_s, ppf	6.5	32.0
Inside/outside fluid, ppg	7.3	-
Weight, ppf	5.8	-
Length, ft	10000	10000
Radial clearance, in	1.610	-
Slack-off, lbf	20000	-

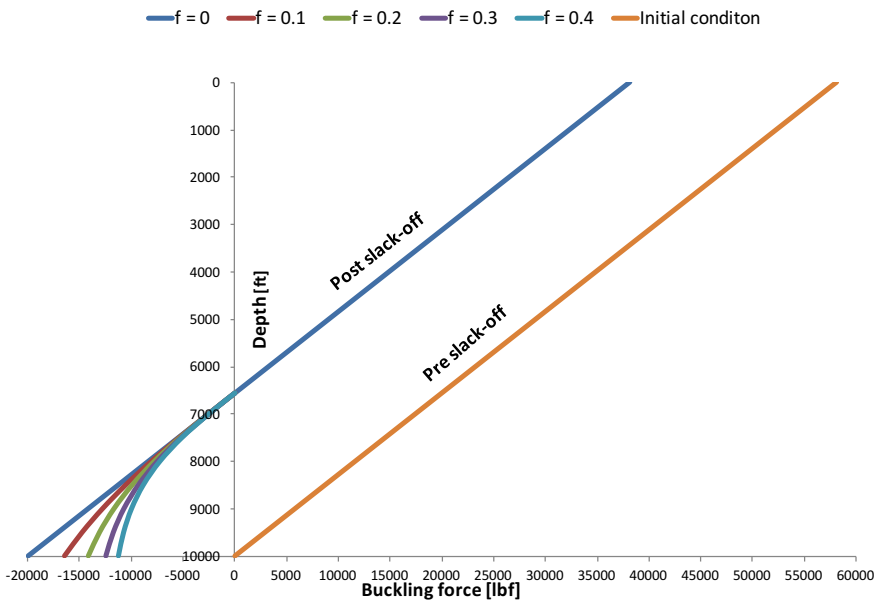

Figure 4.3: Buckling force distribution for 2 7/8 tubing

The curves divert from 6500 feet and downwards, which suggests that the approximate point of neutral stability lies here. Figure 4.3 clearly shows the dramatical effect which friction has on the landing load of the tubing. The landing load is 11200 lbf for f = 0.4, which is only 56% of the applied slack-off load. This can have a significant impact on the drillstring calculations. Similar curves are constructed for the defined drill string in Chapter 5.

4.5.3 Maximum achieveable slack-off force

The maximum slack-off force achieveable by using this method is limited by the buoyed self-weight of the drill string. This can be calculated by setting the neutral point equal to zero and solving for Q in equation 4.26. In other words, this implies that the entire drill string becomes buckled:

$$Q = Lw \tag{4.28}$$

Chapter 5

Case study

This chapter presents a case study designed to test mechanical pre-tensioning of a casing through use of the drill string method. The results of the drill string and casing calculations, and also the corresponding effects on the well design, are presented and discussed in this chapter. The case study is simplified to demonstrate the effects of this method, and the study may therefore not take all well design considerations into account. This approach, however, does not represent an unrealistic design as that would be counterproductive. This case study is made as realistic as possible by basing temperature, well depth, drilling parameters, and material grade selection on published work and results.

5.1 Case study parameters

The case study is based on temperature ranges and well depth ranges encountered along the Tyrrhenian belt in Western-Italy. According to Carella (1999), geothermal gradients may reach 5-20°C/100m (15-61°C/1000 ft), and well depths may extend several kilometers into the subsurface. These ranges may vary depending on the region under consideration.

A 6500 feet deep vertical well having a geothermal gradient of 31°C/1000 ft is considered. Assuming a mean annual air temperature of 15 °C, this gradient produces a reservoir temperature (@ 6500 ft) of approximately 215°C. A 9 5/8", 53.5 ppf, production casing of K55/L80 material is hung off from the wellhead to the base of the well. Two casing grades are under consideration for comparison purposes. The casing is pre-tensioned by a drill string consisting of 5 1/2", 26.48 ppf adjusted weight (21.9 ppf if weight of pipe connections are neglected), S135 drillpipe, and 8", 147 ppf, drill collars with a minimum yield strength of 110 ksi. The grades of the drill pipe and the drill collars are susceptible to change based on the results, and due the risk of hydrogen embrittlement which is a potential failure mode for higher strength grades (Finger & Blankenship 2010). The casing is cemented using 1.43 sg cement, while filled with slightly saline water of 1.03 sg. The drill string is filled and submerged by the the saline water after cementing the casing. All aforementioned (pluss other relevant) parameters are listed in the following tables. The tubuluar properties were found from the following sources.

Drill pipe: WorkstringsInternational® (2015).

Drill collars: Mitchell & Miska (2011).

Casing:Tenaris® (2011).

Table 5.1: Well parameters

	Well
Type	Vertical
Gradient,°C/1000 ft	31
Depth, ft	6500
Res. temp., °C	216.5

Table 5.2: Tubular parameters

	Casing	**Drill pipe**	**Drill collar**
OD, in	9.625	5.5	8
ID, in	8.535	4.778	3
I, in^4	-	19.33	197.09
t, in	0.545	0.361	2.5
OD/t ratio	17.7	15.2	3.2
R, in	-	1.518	0.268
σ_y, ksi	55/80	135	110
E, 10^6 psi	30.45	30.45	30.45
α, 10^{-6} $\frac{1}{^\circ C}$	12	12	12
Length, ft	6500	5960	540
w_s, ppf	53.5	26.48	147
w_i, ppf	25.6	8.0	3.2
w_o, ppf	45.1	10.6	22.5
w, ppf	33.9	23.9	127.7
ρ_i, sg	1.03	1.03	1.03
ρ_o, sg	1.43	1.03	1.03
Q, lbf	211260	-	-211260

5.2 Drill string results

5.2.1 Drill string design

The primary objective of using a drill string as a means of pre-tensioning a casing is solved by using a drill string which is similar or identical to a drill string used to a $12^1/_4$" hole section of a well. This reduces the additional logistics cost. Designing a drillstring is a comprehensive task. The main focus will therefore be to design a drill string capable of:

1. providing sufficient weight-on-bit (WOB) during drilling
2. keeping the equivalent circulating density (ECD) at a minimum
3. fitting inside the $9^5/_8$" casing, while providing sufficient stability to the bottom-hole assembly (BHA) and the drill bit.

Equation (9.1) from Mitchell & Miska (2011) can be used to calculate the required OD of the drill collars to prevent rapid changes in hole deviation. The equation is perhaps more useful for considering inclined wells, but it will in thise case serve as a conservative value allowing for further evaluation.

$$OD_{dc} = 2(OD_{cc}) - OD_{bit} \tag{5.1}$$

For this case, the outer diameter of the casing coupling (OD_{cc}) = 10.625", and the diameter of the bit (OD_{bit}) = 12.25". This gives an OD_{dc} = 9", which is greater than the inside diameter of the casing (8.535"). The OD must be reduced, but not too much. Utilizing a drill collar OD of 8", in combination with a near-bit stabilizer (Mitchell & Miska 2011), should be sufficient for providing the necessary stability of the bit and the BHA.

Reducing the pressure-losses in the drill string is achieved by several means. One such means is to choose a sufficiently large inner flow area of the drill collars. For Newtonian fluids in turbuluent flow, the pressure drop is proportional to the fluid density multiplied by the flow rate squared multiplied by the friction factor. Although more complex relations exist for non-Newtonian fluids, the trends are similar with regards to pressure losses (Aadnoy 2010). It is therefore evident that choosing a relatively large inner diameter of the drill collars will reduce the friction between the inside wall and the cirulating fluids, which leads to reduced pressure losses. Using spiralling drill collars is recommended for drilling areas where differential sticking is a problem. This is usually the case for under-pressured geothermal formations (Finger & Blankenship 2010). The spiral grooves on the outside surface of these drill collars reduce the contact area between the drill collars and the adjacent formations, thereby reducing the risk of differential sticking (Mitchell & Miska 2011). It is the author's understanding that the ECD will be slightly reduced as the annulus flow area increases over the spiral grooves. A published work of this fact has not been found. A spiral drill collar configuration, with minimum ID = 3", is therefore considered sufficient to minimize the ECD and to reduce the chance of differential sticking while drilling.

The required length of the drill collars depends mostly on the desired wieght on bit (WOB). The optimal WOB, in combination with the RPM (revolutions per minute), depends on many

factors, such as rate of penetration (ROP), bit diameter, compressive strength of formations encountered, cuttings control, bit life, etc (Finger & Blankenship 2010) (Mitchell & Miska 2011). As geothermal formations tend to be hard and abrasive (Finger & Blankenship 2010), the required bit weights might exceed what is common in oil and gas wells. As such, it will be assumed an upper fixed value of WOB = 55000 lbf. Equation (9.10) Mitchell & Miska (2011) can be used to calculate the required length of the drill collars based on the maximum expected WOB, and on effective (buoyed) weight of the drill collar:

$$L_{dc} = \frac{(DF)WOB}{w_{dc}} \tag{5.2}$$

Mitchell & Miska (2011) suggests design factors (DF) of 1.15 to 1.20 in nearly vertical holes to ensure that the neutral point of stability lies within the drill collar section. Using $w_{dc} = 127.7$ ppf (see Table 5.2), and assuming a design factor of 1.20, then $L_{dc} = 516.8\ ft$. Assuming that the average length of one joint of drill collar is 30 ft, the required number of joints is 18. This gives $L_{dc} = 18 \cdot 30\ ft = 540\ ft$. Therefore the length of the drill pipe above the drill collars must be: $(6500 - 540)\ ft = 5960\ ft$. Assuming that the whole weight of the drill string is slacked off at the bottom of the well/casing, the pre-tension load generated by each drillstring section is calculated from equation 4.28. The results of the analysis is presented in the following table:

Table 5.3: Drill string design results

	Drill pipe	**Drill collar**
ID, in	5.5	8
OD, in	4.778	3
w, ppf	23.9	127.7
Length, ft	5960	540
Q, lbf	142301	68958

5.2.2 Frictional analysis of a buckled drill string

Two cases were developed for the frictional analysis of a buckled drill string. The first case assumes an average effective weight per unit length along the drill string, thereby effectively neglecting some parameters of the drill collar section. The buyoancy is calculated based on both the drill pipe areas and drill collar areas. Therefore the same slack-off force at the bottom of the drill string is achieved for both cases. The second case takes into account the change of parameters when transitioning from the drill pipe to the drill collar. For the first case, the average effective weight per unit length can be calculated from the following relation:

$$w = \frac{w_{dc} \cdot L_{dc} + W_{dp} \cdot L_{dp}}{L}\ , \tag{5.3}$$

which gives $w = 32.5$ ppf.

Case 1 results are visualized in the following figure.

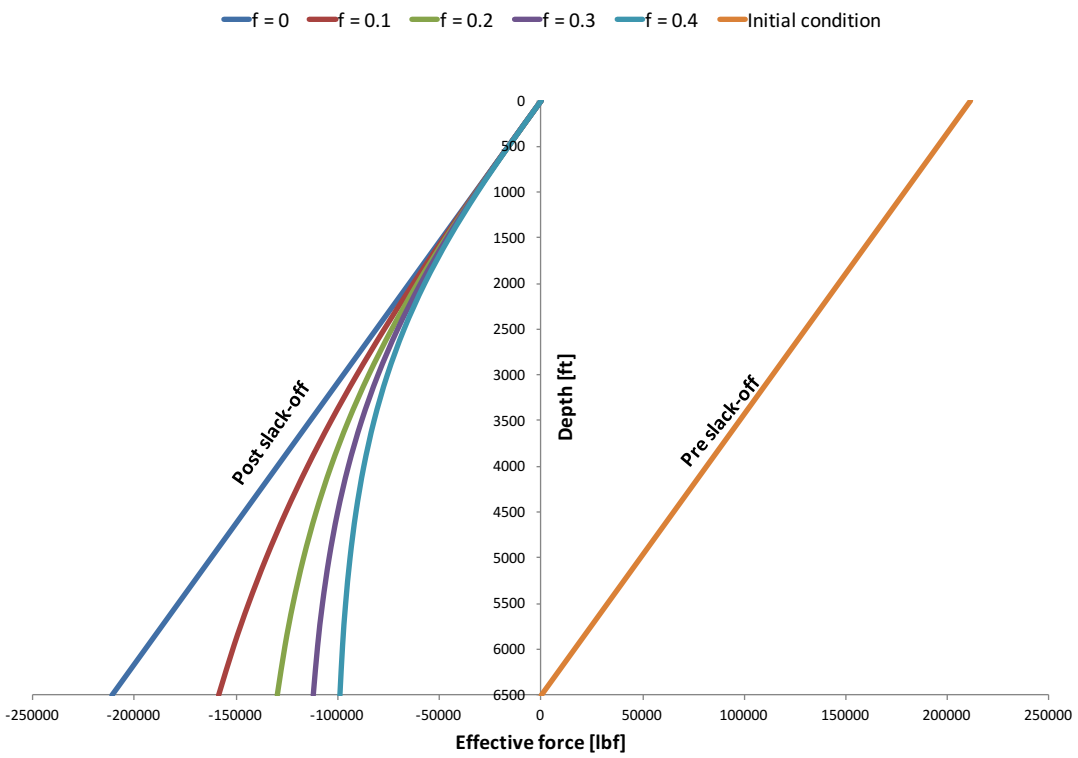

Figure 5.1: Effective force distribution for a 5 1/2" drill pipe without drill collars

The point of interest is at the base of the drill string where the effective force is greatest. At this point, Figure 5.1 shows a considerable effect of friction on the effective force. For f = 0.4 the actual effective force is only 47% of the applied slack-off force (Q = 211260 lbf). However, this representation is simplified and therefore less accurate.

When considering the parameters in Table 5.2, it is evident that the radial clearance (R), moment of inertia (I), and the effective weight per unit length (w) changes drastically in the transition area from the drill pipe to the drill collar in the drill string. The parameters that greatly affect the friction results are moment of inertia (a ten-fold increase) and weight per unit length (a six-fold increase). This can be seen when considering equations 4.25 and 4.27.

Case 2 results are visualized in the following figure.

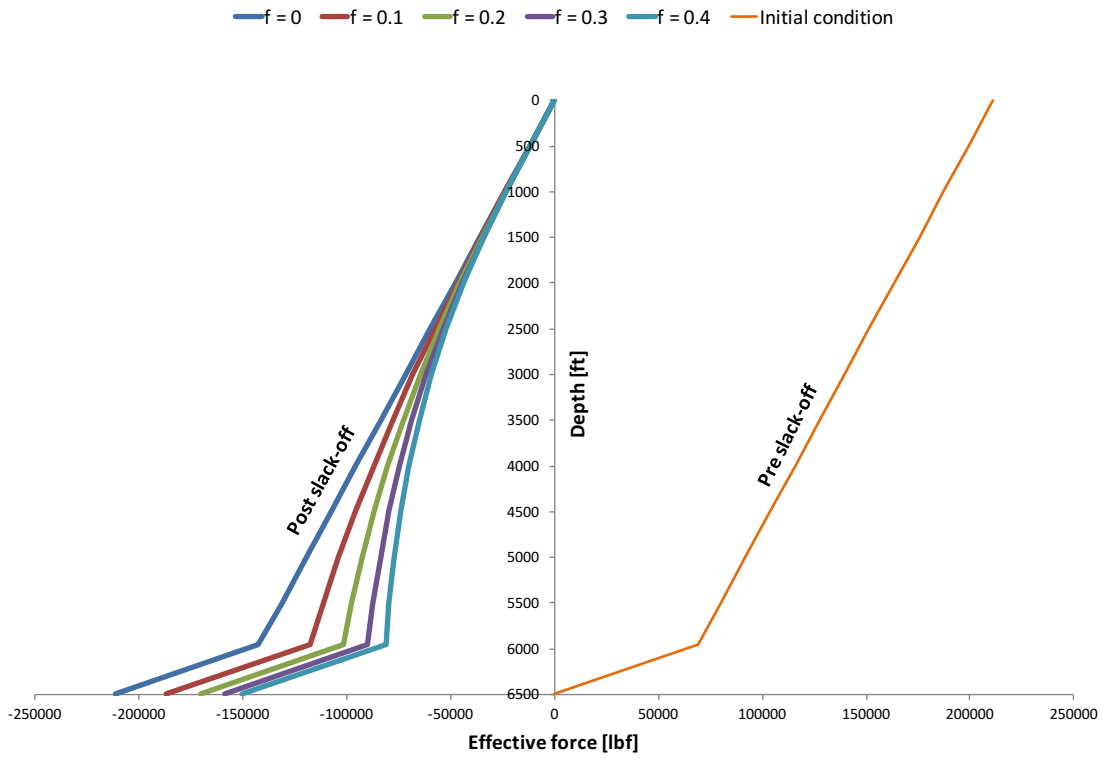

Figure 5.2: Effective force distribution for a $5\,{}^{1}/_{2}''$ drill pipe with drill collars

Although Figure 5.2 is not as visually appealing as the former, it represents a more realistic scenario. The buoyed weight per unit length is calculated individually for each of the drill string sections by using equation 4.24. See Table 5.2 for specific values.

Consider the base of the drill string for f = 0.4 in Figure 5.2. The effective force is 71% of the applied slack-off force, which is 24% more than what is predicted in Figure 5.1. The results suggest that the friction factor plays a lesser role in the drill collar section and are instead dominated by the increase in I and w, and a decrease in R. Although different results, both cases show a similiar trend: increased friction between the casing and the drill string reduces the effective force on the drill string. It is evident from both figures that the most severe load on the drill string is the case of no friction. This scenario is pursued in the following analyses.

The results of the friction analysis is summarized in the following table. Abbreviation list:

- DS = drill string
- DC = drill collar
- w/ = with
- w/o = without
- Q = applied slack-off force (-211260 lbf)

Table 5.4: Frictional analysis results

f	DS w/ DC [lbf]	% of Q	DS w/o DC [lbf]	% of Q
0	-211260	100	-211260	100
0.1	-186586	88	-158701	75
0.2	-170348	81	-130055	62
0.3	-158802	75	-111881	53
0.4	-150145	71	-99237	47

5.2.3 Real and effective forces in drillstring

Equation 4.1 simply cannot be used for calculating the real force when considering advanced geometries. This is the case for a drill string with drill pipe and drill collars, where piston forces are present at the internal and the external shoulder of the drill pipe-to-drill collar transistion area.

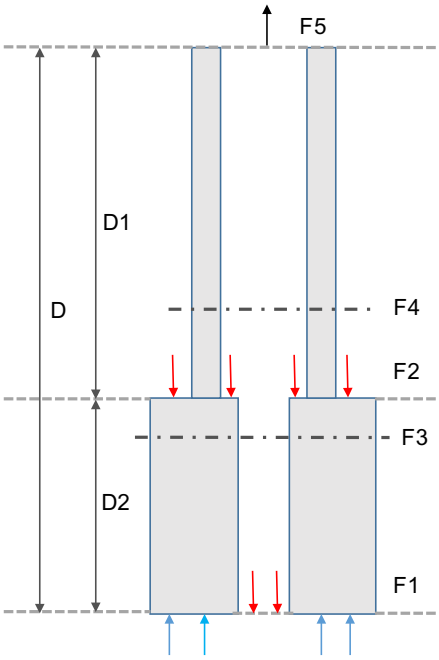

Figure 5.3: Piston forces the in drill string

Figure 5.3 shows the axial forces and the piston forces in a combined drill string. Some explanation is required. The thicker bottom part of the figure represents the drill collar section, while the thinner upper part represents the drill pipe section. F1 represents the resultant hydraulic force pushing upwards at the bottom of the drill collars. This force is represented by the resultant magnitude of blue arrows pointing upwards at the bottom of the drill string, and the red arrows pointing downwards at the bottom of the drill string. F2 represents the downward hydraulic force in the drill collar/drill pipe transistion area. This force is represented by the red arrows working downwards on the exposed external and

internal shoulder of the drill collar section. F3 represents the force at the top of the drill collars, and F4 represents the force at the bottom of drill pipe. F5 is the force at top of the drill string. D1, D2 and D represent the section length of the drill pipe, the drill collar, and the drill string, respectively. Blue and red arrows symbolize the direction of forces. Blue = upwards = negative, while red = downwards = positive. Using the approach described in Section 4.5 of Aadnoy (2006), and considering the same density of the fluid on the inside and the outside of the drill string, the following can be derived:

$$F1 = -P_o(D)A_{o,dc} + P_i(D)A_{i,dc} = \underline{-P(D)A_{s,dc}}$$

$$F2 = P(D1)(A_{o,dc} - A_{o,dp}) + P(D1)(A_{i,dp} - A_{i,dc}) = \underline{P(D1)(A_{s,dc} - A_{s,dp})}$$

$$F3 = \underline{F1 + w_{s,dc} \cdot D2}$$

$$F4 = \underline{F3 + F2}$$

$$F5 = \underline{F4 + w_{s,dp} \cdot D1}$$

The above formulations represent the initial condition of the drill string, where the drill string is in tension. Once slacked-off, each segment must include the slack-off load Q.

As stated by Aadnoy (2006), hydrostatic loading does not govern failure. Deviatoric loading, or effective force, govern failure. Therefore the average hydrostatic force at each point considered must be subtracted from the total load, or the real force. Derivation of the effective force is not included here, but the derivation has been performed by Aadnoy (2006). The result, however, is quite simple. The effective force is equal to the effective (buoyed) unit weight multiplied by the length of steel up to the point of interest, which is usually the top of the drill string or the top of the drill collar section (if using the bottom of well as a datum).

With the above paragraphs in mind, the following figure graphically represents the real and effective forces in the drill string.

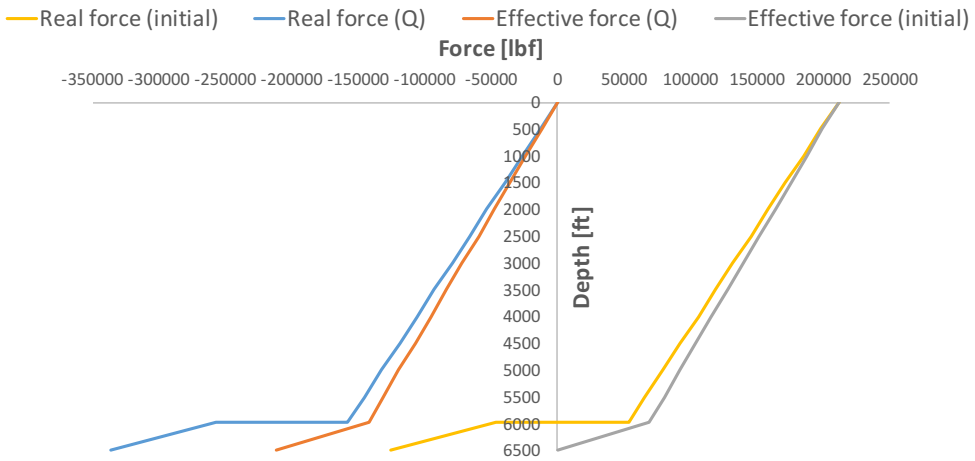

Figure 5.4: Real and effective forces in the drill string

The initial condition of the drill string is taken to be the condition of the drill string after the cementing operation, but prior to the engagement of the mechanical slips. The drill string is therefore in tension at top. The condition of the drill string during slack-off is denoted Q., the condition at which the whole drillstring is in compression. Figure 5.4 serves as an input to the following stress analysis.

5.2.4 Stress analysis of the drill string

The stress calculations become considerably simplified if the fluid on the inside and outside of the drill string has the same density. Under this hydrostatic condition, the radial and tangential stress become:

$$\sigma_r = \sigma_t = -P \quad .$$

This results in a simplified expression for the Von Mises stresses:

$$\sigma_{VME} = |\sigma_z + P|$$

All stresses are plotted against well depth in the following figure. The mathematical terms in equations 4.3 and 4.4 that consider the stress distribution across the wall thickness become zero under the condition of equal pressure on the inside and the outside of the drill string. Yielding, if any, can therefore start at either wall.

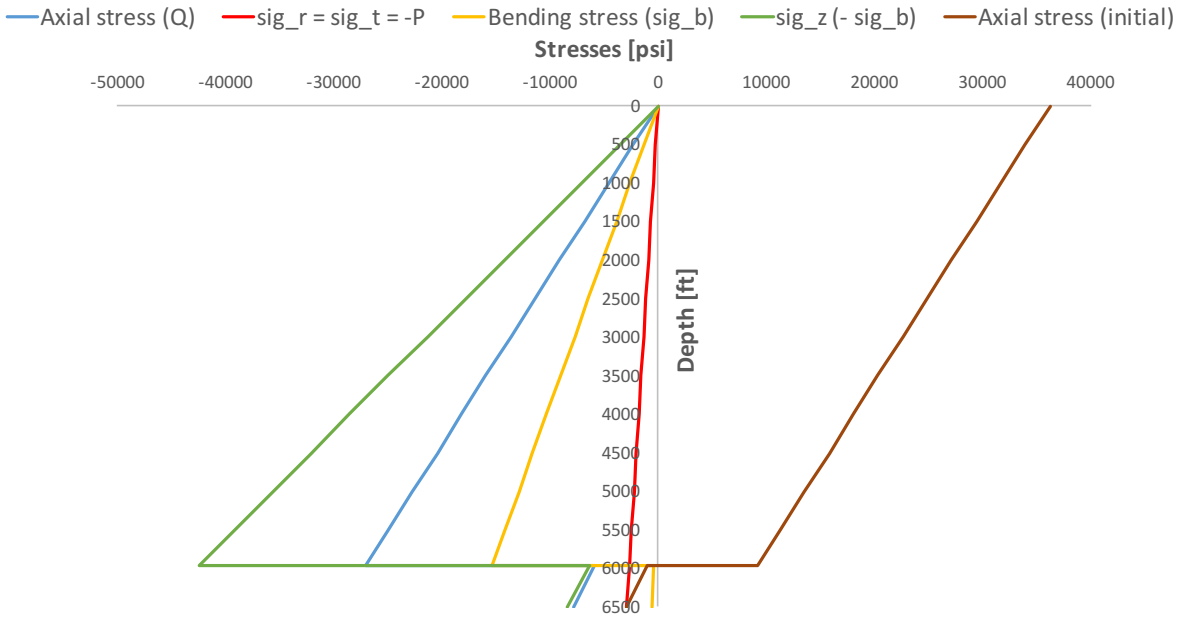

Figure 5.5: Stresses in the drill string

For reference: "initial" and "Q" in paranthesis in the legend of the graphs represent intial and slack-off conditions, respectively. sigb is the Excel representation of the bending stress, σ_b. Note the considerable change in stresses at approximately 6000 ft. One would intuitively expect the stresses to be greatest where the slack-off force is at maximum, which is at the bottom of the drill string. However, the increased area of steel and a ten-fold increase in the moment of inertia when transitioning from drill pipe to drill collar, result in minimized stresses. Clearly, the drill collar section has a significant impact on the performance of the drill string. The same message is conveyed in the following figure.

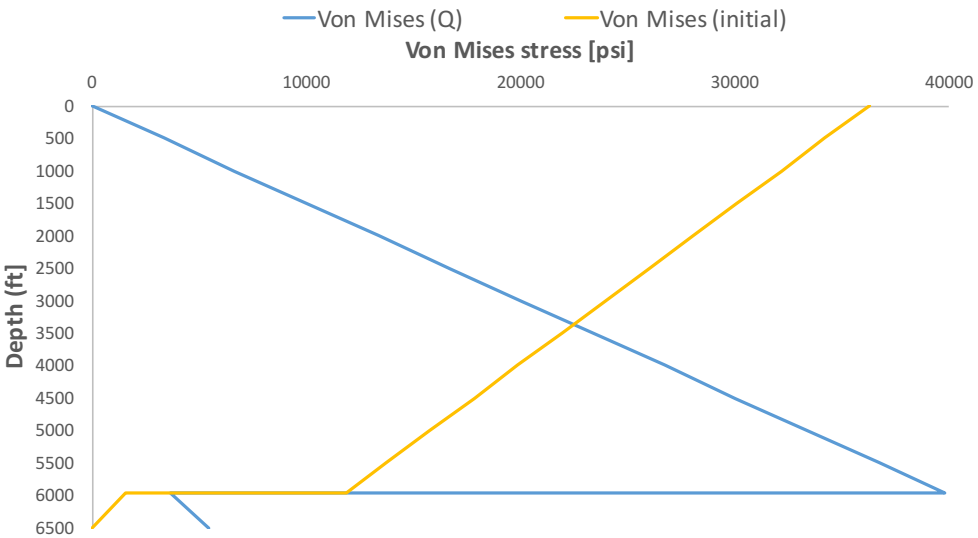

Figure 5.6: Von Mises stresses in the drill string

As can be seen in Figure 5.6, the point of greatest stress is at the bottom of the drill pipe section at 5960 ft. Actually, there is not much difference between the Von Mises stresses at the top of drillstring when in the intial condition, and the stresses at the bottom of the drill pipe after slack-off. The main difference is that, initially, the whole weight of the drill string is in tension at the top. Thus the weight of the drill collars are also included. After slack-off, however, the combined compression and bending forces at the bottom of the drillpipe section exceed the tensile force at the top of drill string.

The main conclusion is that therefore the bending stresses due to helical buckling are quite significant at the bottom of the drill pipe. This is also evident when studying Figure 5.5. In fact, the absolute value of σ_z exceeds σ_{VME}. The design factor for both situations are calculated. It is now assumed that the bottom of the drill pipe holds a temperature of 100°C, and that the yield strength deration follows that of L80/C90/T95 casing grades as represented in Table 4.1. The percentage-of-yield at the point of greatest stress then becomes:

Von Mises

$$\%-yield = \frac{39773}{135000 \cdot 0.96} \cdot 100\% = \underline{\underline{30.7\%}}$$

Or, utilizing the definition of the design factor (DF):

$$DF = \frac{100\%}{\%-yield} = \underline{\underline{3.26}}$$

Total axial stress

$$\%-yield = \frac{|-42435|}{135000 \cdot 0.96} \cdot 100\% = \underline{\underline{32.7\%}}$$

Or, utilizing the definition of the design factor (DF):

$$DF = \frac{100\%}{\% - yield} = \underline{\underline{3.05}}$$

It is clear that the drillstring will not permanently corkscrew (yield) under its own self weight and its buckling-induced bending stresses, whereby lower material strength of drill pipe may be selected.

5.3 Casing results

5.3.1 Cement design

Geothermal well conditions impose challenging environments for the cement, thereby making it correspondingly difficult to preserve cement integrity throughout the life of the well. The cement must withstand low pH-values (due to the presence of H2S gas), highly corrosive brines and fluids (CO2 and formation fluids up to 10 times total dissolved solid content than sea water (Finger & Blankenship 2010)), and high temperatures. The cement density must be carefully selected such as to avoid circulation losses through the usually under-pressurized and highly fractured formations (Finger & Blankenship 2010).

Brookhaven National Laboratory developed, with support from Halliburton, Unocal Operation, and CalEnergy Operating Corporation, a non-Portland cement designed to withstand the harsh conditions imposed on geothermal well cements (Sugama 2006). The cement is usually abbreviated as CaP (calcium aluminate phosphate). The cement met all the requirements set by the industrial partners, including achieving foamed cement densities lower than 1.3 s.g (10.85 ppg). One of the shortcomings from lowering the cement density by airation was, however, the reduction of water permeability "due to the formation of an undesirable continuous porous structure caused by coalesced air bubble cells" Sugama (2006). Higher water permeability would undesireably lead to elevated corrosion rates of the casing.

A series of waterborne acrylic-based polymer additives were incorporated, and results showed a significantly improved corrosion-preventing behaviour of the air-foamed CaP cement. The polymer which showed the best performance was styrene acrylic emulsion (SAE). Interestingly, the incorporation of SAE further reduced the cement slurry density (Sugama 2006).

In 1999, Halliburton commercialized this cement under the tradename ThermaLock Cement®. Of 2006 this cement has been used to complete geothermal wells in Indonesia, Japan and United States (Sugama 2006). The design of cement for this case study is therefore based on CaP cement developed by Brookhaven National Laboratory. The cement properties are based on Table 2 Sugama (2006), which is the unmodified (no polymer added) version of air-foamed CaP cement. Do note that the results are based on air-foamed CaP cement autoclaved at 200°C. The autoclave is a pressure chamber used to carry out processes at elevated temperature and pressure. The cement property of interest in this analysis is the slurry density, **1.43 sg**. This density is obtained by incorporating 3 weight percent of foaming reagent into the CaP slurry.

5.3.2 Stress analysis of the casing

The real forces in casing are much simpler to calculate compared to the drill string as there are no internal or external shoulders in the casing as uniform inner and outer area of casing is considered. There are only piston forces acting at the bottom of the casing. In such a simple case, equation 4.1 can be used. Also, as there are no bending stresses in the casing ($\sigma_b = 0$), the total axial stress equals the axial stress ($\sigma_z = \sigma_a$), which is governed by the real force. As such, effective forces are not of interest when considering the axial performance of the casing under pre-tensioning load Q. The real force before pre-tensioning ("initial" in legend of graph), and post pre-tensioning ("Q" in legend of graph), are visualized in the following figure.

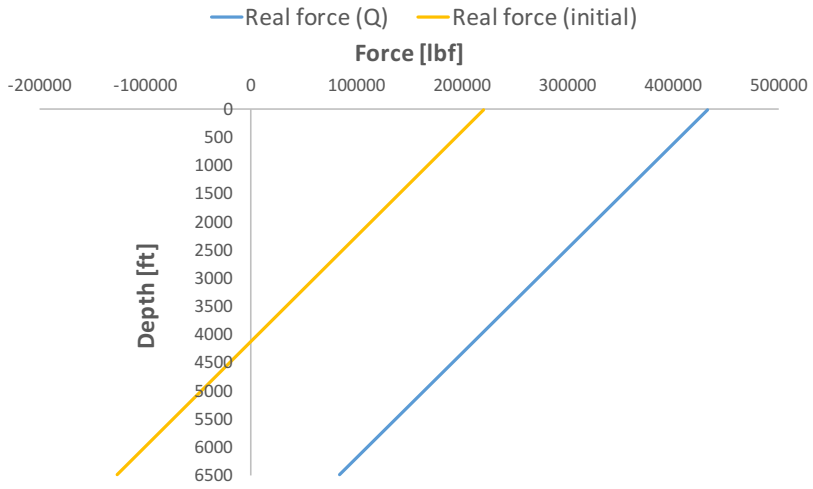

Figure 5.7: Forces in the casing

Figure 5.7 serves as an input to the following stress analysis of the casing. Note that the difference between the two curves is the applied pre-tension load Q.

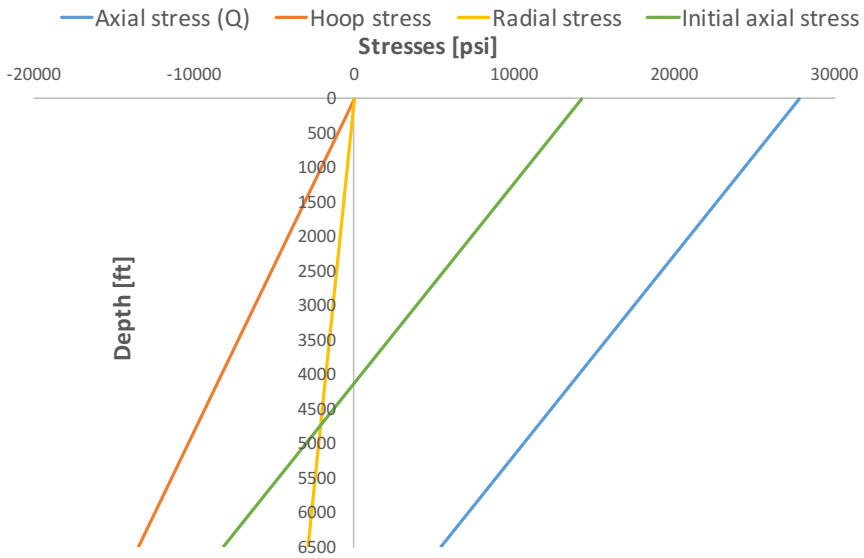

Figure 5.8: Stresses in the casing

Consider Figure 5.8. As expected, the axial stresses are greatest at the top of the casing under pre-tension load Q. Naturally, the same is concluded in the following figure of the Von Mises stresses in the casing.

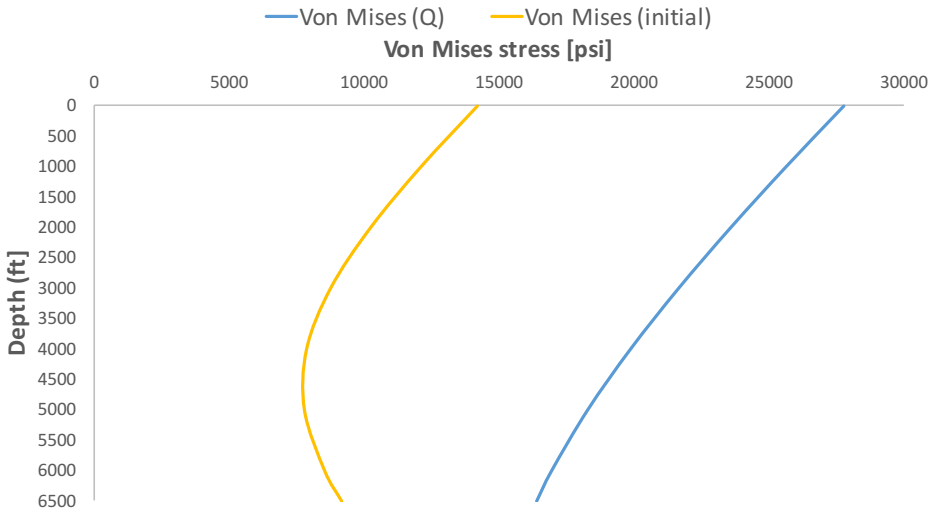

Figure 5.9: Von Mises stresses in the casing

The slightly bent shape of these curves is due to the upward compressive effect of the higher density fluid on the outside of the casing. The blue curve is bent less due to the downward tensile force from the applied pre-tension load counteracting the compressive effect. In any case, the point of interest is at the top of the casing of the blue curve where the Von Mises stresses are the greatest. Under the assumption that the maximum expected temperature at the top of the casing equals the reservoir temperature (215°C), and that the yield strength deration follows that of Table 4.1, the following percentage-of-yield and design factor at the point of greatest stress are obtained. Linear interpolation is used to obtain exact yield strength deration factors.

K55 casing

$$\%-yield = \frac{27775}{55000 \cdot 0.885} \cdot 100\% = \underline{\underline{57.1\%}}$$

$$DF = \frac{100\%}{\%-yield} = \underline{\underline{1.75}}$$

L80 casing

$$\%-yield = \frac{27775}{80000 \cdot 0.894} \cdot 100\% = \underline{\underline{38.8\%}}$$

$$DF = \frac{100\%}{\%-yield} = \underline{\underline{2.57}}$$

For the casing grades under consideration, it is evident that they will not yield in tension under the pre-tension load Q. Interestingly, NZS 2403:2015 (2015) recommend a minimum design factor of 1.80 when considering tensile force during running and cementing of a casing. Only the L80 casing satisfies this recommendation. An important note is observed concerning the temperature for the K55 casing: As it has been shown in Chapter 4, a fully cemented-to-surface K55 casing will under normal circumstances yield at a temperature differential of 150°C. The differential temperature at the top of the casing is actually 200°C if the reference temperature of the cement at this point is assumed to be 15°C, which would cause this casing to yield due to thermally-induced compressive stresses. The above analysis is based on the tensile forces in the casing during cementing while applying pre-tensioning from drill string. As a conservative value, the yield strength is derated for a production scenario. Therefore the above design factors are also conserative. The following section discusses the differential temperatures at which the two casings can operate before and after the pre-tensioning.

5.4 Effect of pre-tensioning on the casing temperature range

5.4.1 Production scenario

Any pre-tension load applied on the casing will increase its temperature range during heating/production, as the additional tensile forces counteract the thermally-induced compressive forces. The following figure shows the additional temperature differential ($\triangle T_{pt}$) obtained as a function of pre-tension load Q.

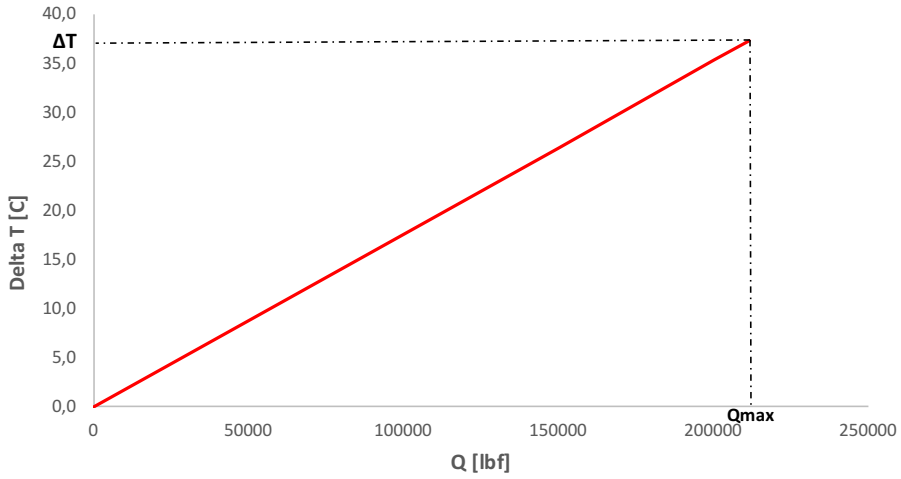

Figure 5.10: Increased temperature range during production

Q_{max} is the maximum achieveable pre-tension load that can be transferred from the drill string to the casing. Under this load, the increased temperature differential equals **37°C**. The dashed lines are used to illustrate the position of these parameters on their respective axes.

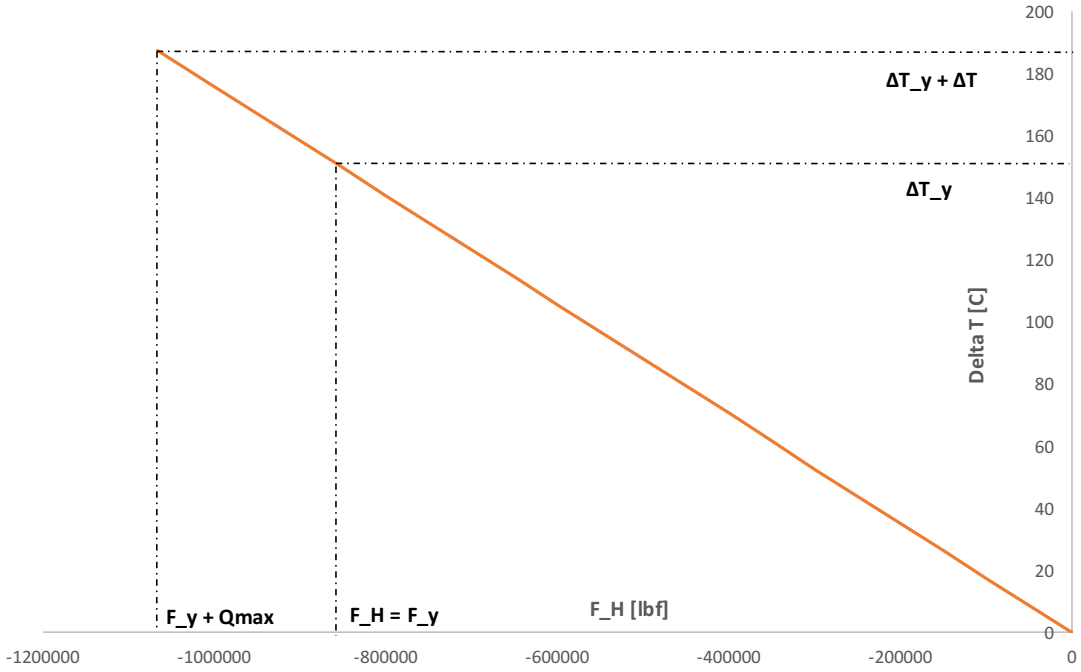

Figure 5.11: Temperature range of a K55 casing during production after pre-tensioning

Consider the above Figure 5.11. F_H represents the compressive forces in the casing during production, and these compressive forces are assigned negative values. F_y is the compressive force that causes the casing to yield under no pre-tension load, while $F_y + Q_{max}$ is the compressive force that causes yielding under the pre-tension load Q_{max}. Correspondingly, $\triangle T_y$ is the temperature differential that causes yielding under no pre-tension load, and $\triangle T_y + \triangle T_{pt}$ is the temperature differential that causes yielding under the pre-tension load Q_{max}. Prior to pre-tensioning, the casing yields at $\triangle T = 150°C$. After pre-tensioning, the casing yields at $\triangle T = 188°C$, which corresponds to a 25% increase in the temperature. For the case defined herein, it is not sufficient to consider a 53.5 ppf K55 casing for a stress-based design as maximum expected temperature differential (now denoted $\triangle T_{max}$) equals 200°C. The casing will yield. Disregarding the fact that the K55 casing would yield under the temperature differential considered here, it is evident that the pre-tensioning of the casing has a significant positive impact on its operating range during production.

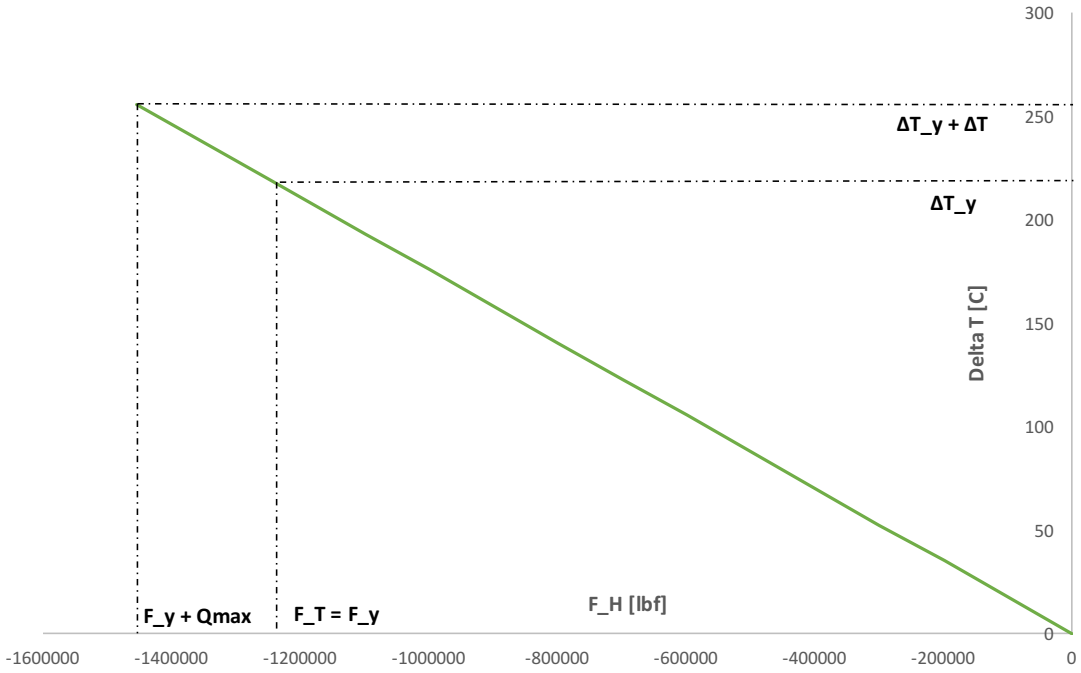

Figure 5.12: Temperature range of a L80 casing during production after pre-tensioning

Figure 5.12 shows the temperature range of a 53.5 ppf L80 casing during production after pre-tensioning. The only difference between the K55 and L80 casing is the increased yield strength, which leads to a higher operating range for the L80 casing. The maximum differential temperature that the L80 casing can be subjected to before yield therefore increases from 219 to 256°C. A L80 casing must be used to ensure a safe well design for the case defined herein.

5.4.2 Cooling scenario

Any pre-tension load applied on the casing will decrease its temperature range during cooling, as the additional tensile force acts together with the thermally-induced tensile force. The following figure shows the reduced temperature differential ($\triangle T_{pt}$) obtained as a function of pre-tension load Q.

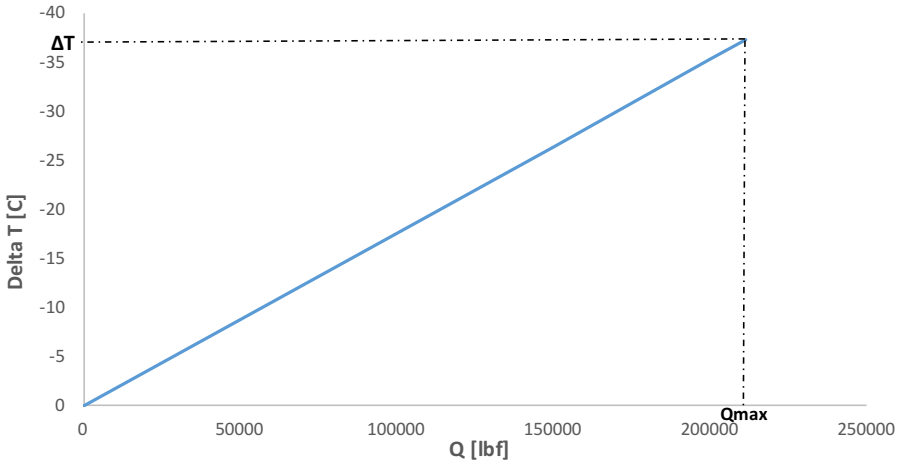

Figure 5.13: Decreased temperature range during cooling

Notice the negative value of $\triangle T$ along the y-axis of Figure 5.13. A pre-tension load of Q_{max} will decrease the operating range of casing during cooling to **- 37°C**, which is the opposite of what is presented under sub-section 5.4.1. Ultimately, this makes the well design more sensitive to negative temperature differentials, which is the case for well quenching.

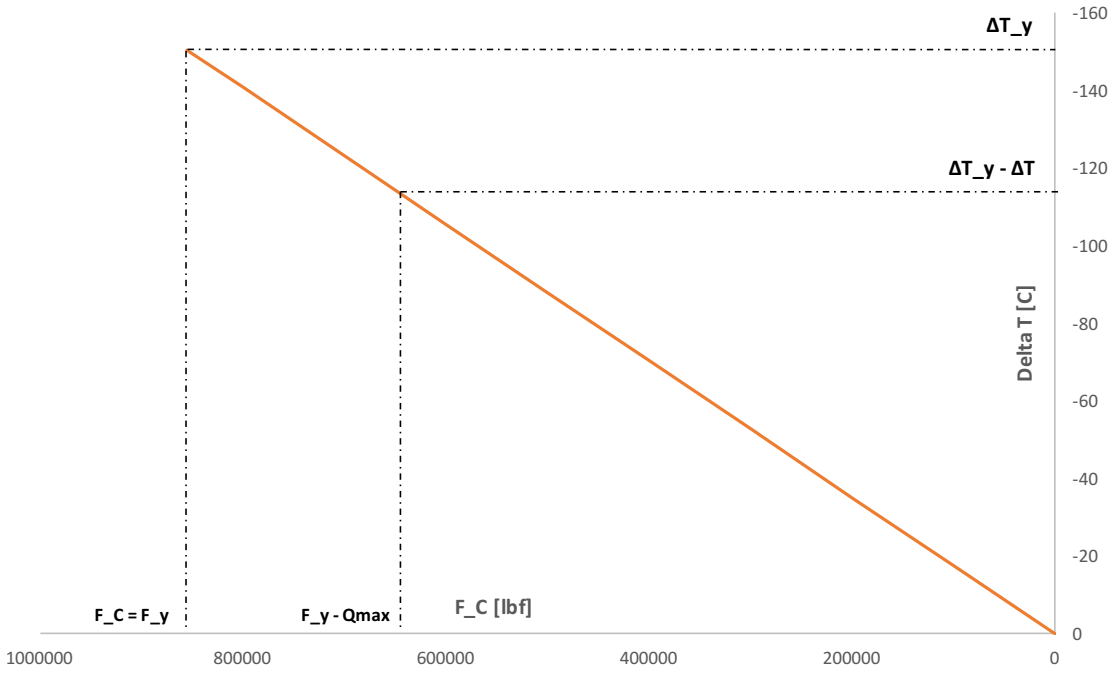

Figure 5.14: Temperature range of K55 casing during cooling after pre-tensioning

Consider the above Figure 5.14. F_C represents the tensile forces in the casing during cooling, and these tensile forces are assigned positive values. F_y is the tensile force that causes the casing to yield under no pre-tension load, while $F_y - Q_{max}$ is the tensile force that causes yielding under the pre-tension load Q_{max}. Correspondingly, $\triangle T_y$ is the temperature differential that causes yielding under no pre-tension load, and $\triangle T_y - \triangle T_{pt}$ is the temperature differential that causes yielding under pre-tension load Q_{max}. Prior to pre-tensioning, the casing yields in tension at $\triangle T = -150°C$. After pre-tensioning, the casing yields in tension at $\triangle T = -113°C$, which corresponds to a 25% decrease in the temperature. The temperature range for a L80 casing during cooling decreases from $\triangle T = -219°C$ to $\triangle T = -182°C$. This is shown in the following Figure 5.15.

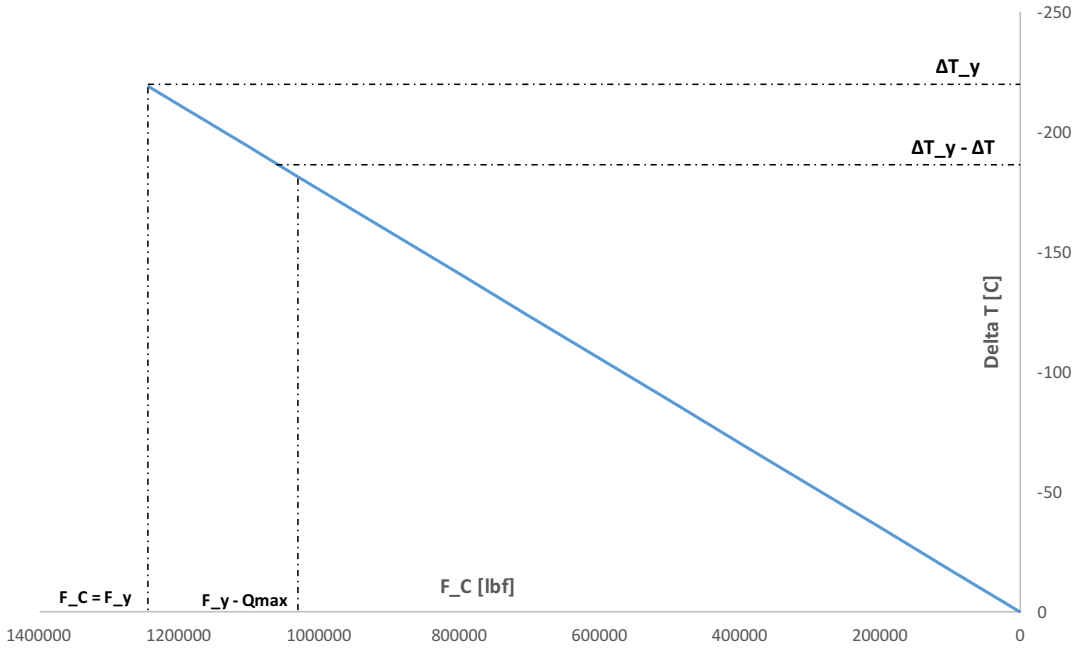

Figure 5.15: Temperature range of L80 casing during cooling after pre-tensioning

5.5 Summarized results of case study

The case study results are summarized in the following table. The results show the temperature differentials that the casing can tolerate under production (heating) and cooling, before and after pre-tension load Q has been applied. The design factors for both casings and the drill pipe are presented.

Table 5.5: Summarized case study results

	Before Q [°C]		**After Q [°C]**		
Tubular	Heating	Cooling	Heating	Cooling	DF
K55 casing	150	-150	188	-113	1.75
L80 casing	219	-219	256	-182	2.57
S135 drillpipe	-	-	-	-	3.05/3.26

5.5.1 Key findings

Based on the results presented in the aforementioned table and analyses, the following key findings result from this case study:

1. Drillpipe nor casings will yield under a slack-off/pre-tension load Q.
2. Therefore, the maximum achieveable slack-off/pre-tension force provided by the drill-string becomes the limitation. This force can be increased by designing a drill string with a longer than normal drill collar section, or simply by designing a longer drillstring as a function of wellbore vertical depth.
3. Increased friction between the casing and the buckled drillstring reduces the effective force on the drill string, resulting in greater operational margins.
4. Lower grade drillpipe can be a viable and cheaper option for performing casing pre-tensioning as analyse show that calculcated design factors based on maximum stress concentration in drill pipe during operation are far from causing failure of the drill pipe.
5. The design factor for a L80 casing comply with recommendations by NZS 2403:2015 (2015).
6. Compressive forces that arise during production of hot fluids in geothermal production casings can potentially lead to failure in the casing body and/or casing couplings. It has been shown that, by pre-tensioning the casings, the casings temperature range during production is increased as the pre-tensile forces reduce the probability of compressional failure.
7. It has been shown that casings are subject to decreased temperature performance during cooling after being pre-tensioned. Caution must therefore be exercised when cooling a pre-tensioned well.

Chapter 6

Conclusion

A novel pre-tensioning method is presented in this thesis. A pre-tension load is initialized by slacking-off a drill string mechanically engaged to a casing during the cementing of a geothermal production casing. Performing cementing and pre-tensioning of this casing simultaneously in the same run reduces operational time. Pre-planning this operation can prove useful when the drillstring design takes both drilling and pre-tensioning into consideration. This leads to optimized logistics.

A simplified case study of a 6500 ft deep, vertical well was constructed to test the feasibility, the limitations, and the effect of this pre-tensioning method on the operational temperature range of geothermal production casings. The results showed that the maximum achieveable pre-tension load on the drillstring would not cause yield in either of the two casings considered, nor in the drillstring itself. In fact, design factors suggest that each of the casings could be pre-tensioned even further without causing failure. As such, the drill string can be made heavier by designing a longer drill collar section so as to increase the pre-tension load on the casings.

In a production scenario, the maximum pre-tension load considered increased the temperature range of casings by 37°C. This corresponds to a 25% increase in temperature performance for a 53.5 ppf K55 production casing. The increased temperature performance reduces the risk of rapid heat-up failure in the casing body and/or casing couplings, a problem commonly encountered during production start up. If high temperature is the contributing factor to failure, inducing a pre-tension load on critical casings could lead to a safer design, and could provide potential savings in optimizing the material grade selection.

The tensile forces added to the casing by virtue of pre-tensioning reduced the temperature range by 37°C in a cooling scenario. As such, great caution must be exercised when considering cooling down a pre-tensioned well. Measures that reduce the need to kill the well by injecting cold water are highly recommended, not only to promote the use of pre-tensioning, but also because repeated thermal cycling of casings cause failure and inevitably leads to a reduced well life.

One of the main parameters which govern the maximum applicable pre-tension load on the casing by use of the drill string is the vertical depth of the well. This method is therefore mainly aimed at moderately deep geothermal wells that extend several kilometers into the subsurface. Should the depth and design allow it, the method could also be of interest for high-temperature gas and steam injection/cyclic steam injection wells. If considering to use this method for shortwer wells, the weight per unit length of the drill string must be doubled

or tripled to achieve an appreciable effect on the well. The drill string would mainly consist of big and heavy drill collars, which are time-consuming to make and break.

The main focus of the casing analyses of this case study was to identify the axial performance of casings after applying a pre-tension load. Other effects, such as the casing burst and collapse performance after pre-tensioning, have not been investigated and are therefore subject to further research. Larger sized production casings ($10\frac{3}{4}$" and $13\frac{5}{8}$"), well inclination, shear strength considerations between the cement sheath and the casing, and also mechanical slip design, are potential candidates for further work.

References

Aadnoy, B. S. (2006), *Mechanics of drilling*, Shaker.

Aadnoy, B. S. (2010), *Modern well design*, CRC Press.

Bellarby, J. (2009), *Well completion design*, Vol. 56, Elsevier.

Birkisson, S. F. & Hole, H. (2006), Aerated fluids for drilling of geothermal wells, *in* 'European Geothermal Congress', Vol. 30.

Carella, R. (1999), 'Italian geothermal district heating systems', http://www.oit.edu/docs/default-source/geoheat-center-documents/quarterly-bulletin/vol-20/20-4/20-4-art5.pdf?sfvrsn=4. [Accessed: 11.06.2016].

eia.gov (2015), 'Use of geothermal energy', http://www.eia.gov/energyexplained/index.cfm?page=geothermal_use. [Accessed: 12.06.2016].

Finger, J. & Blankenship, D. (2010), 'Handbook of best practices for geothermal drilling', *Sandia National Laboratories, Albuquerque* .

Friðleifsson, G. Ó., Pálsson, B., Albertsson, A. L., Stefánsson, B., Gunnlaugsson, E., Ketilsson, J. & Gíslason, Þ. (2015), Iddp-1 drilled into magma–world's first magma-egs system created, *in* 'World Geothermal Congress'.

H. Dickson, M. & Fanelli, M. (2004), 'What is geothermal energy?', http://www.geothermal-energy.org/what_is_geothermal_energy.html#c260. [Accessed: 12.06.2016].

Hole, H. (2008), Geothermal well design–casing and wellhead, *in* 'Petroleum Engineering Summer School. Dubrovnik, Croatia. Workshop', Vol. 26.

Holligan, D., Cron, C., Love, W., Buster, J. et al. (1989), Performance of beta titanium in a salton sea field geothermal production well, *in* 'SPE/IADC Drilling Conference', Society of Petroleum Engineers.

Holmquist, J., Nadai, A. et al. (1939), A theoretical and experimental approach to the problem of collapse of deep-well casing, *in* 'Drilling and Production Practice', American Petroleum Institute.

Huenges, E. & Ledru, P. (2011), *Geothermal energy systems: exploration, development, and utilization*, John Wiley & Sons.

Li, Z.-F. (2008), 'Casing cementing with internal pre-pressurization for thermal recovery wells', *Journal of Canadian Petroleum Technology* **47**(12).

Lubinski, A., Althouse, W. et al. (1962), 'Helical buckling of tubing sealed in packers', *Journal of Petroleum Technology* **14**(06), 655–670.

Lubinski, A. et al. (1950), A study of the buckling of rotary drilling strings, *in* 'Drilling and Production Practice', American Petroleum Institute.

Magneschi, P., Bagnoli, C., Lazzarotto, A. & Ricciardulli, R. (1995), 'Structural models for the analysis of stresses in the casing of geothermal wells', http://www.geothermal-energy.org/pdf/IGAstandard/WGC/1995/2-Magneschi.pdf. [Accessed: 13.06.2016].

Mitchell, R. (1986), Simple frictional analysis of helical buckling of tubing. spe drill eng 1 (6): 457–465, Technical report, SPE-13064-PA. ht tp://dx. doi. org/10.2118/13064-PA.

Mitchell, R. F. & Miska, S. Z. (2011), *Fundamentals of drilling engineering*, Richardson, TX.: Society of Petroleum Engineers.

Mitchell, R. F. et al. (2003), The twist and shear of helically buckled pipe, *in* 'SPE/IADC Drilling Conference', Society of Petroleum Engineers.

Nelson, E. B. & Guillot, D. (2006), *Well cementing*, Schlumberger.

NZS 2403:2015 (2015), *Code of practice for deep geothermal wells*, Standards Association of New Zealand.

petrowiki.org (2015), 'Casing and tubing buckling', http://petrowiki.org/Casing_and_tubing_buckling. [Accessed: 13.06.2016].

Shigley, J. E. (2011), *Shigley's mechanical engineering design*, Tata McGraw-Hill Education.

Southon, J. N. (2005), Geothermal well design, construction and failures, *in* 'Proceedings World geothermal congress', p. 2.

Sugama, T. (2006), 'Advanced cements for geothermal wells', *Brookhaven Science Laboratories under Contract No. DEAC02-98Ch10886 with the US Department of Energy* .

Tenaris®(2011), 'Pipe body performance properties catalogue', http://www.tenaris.com/en/MediaAndPublications/BrochuresAndCatalogs/OCTG.aspx. [Accessed: 11.06.2016].

Thorhallsson, S. (2003), 'Geothermal well operation and maintenance', *IGC2003 Short Course, Geothermal Training Programme, The United Nations University, Iceland* pp. 195–217.

Timoshenko, S. & Goodier, J. (1970), 'Theory of elasticity (3rd edit.) mcgraw-hill', *New York* .

WorkstringsInternational®(2015), 'Spec sheet for s-135 drill pipe', http://workstringsinternational.com/pdf/specs/drill_pipe/us/WS41-01_DPPS.pdf. [Accessed: 11.06.2016].